Basin Research (2001) **13,** 217–238

Evolution of the intracratonic Officer Basin, central Australia: implications from subsidence analysis and gravity modelling

D Haddad,* A. B. Watts* and J. Lindsay†

**Department of Earth Sciences, University of Oxford, Parks Road, Oxford, UK*

†Research School of Earth Sciences, Australian National University, Canberra, ACT, Australia

ABSTRACT

The intracratonic basins of central Australia are distinguished by their large negative Bouguer gravity anomalies, despite the absence of any significant topography. Over the Neoproterozoic to Palaeozoic Officer Basin, the anomalies attain a peak negative amplitude in excess of 150 mGal, amongst the largest of continental anomalies observed on Earth. Using well data from the Officer and Amadeus basins and a data grid of sedimentary thicknesses from the eastern Officer Basin, we have assessed the evolution of these intracratonic basins. One-dimensional backstripping analysis reveals that Officer and Amadeus basin tectonic subsidence was not entirely synchronous. This implies that the basins evolved as discrete geological features once the Centralian Superbasin was dismembered into its constituent basins. Two- and three-dimensional backstripping and gravity modelling suggest that the eastern Officer Basin evolved from a broad continental sag into a region of intracratonic flexural subsidence from the latest Neoproterozoic, when flexure of the lithosphere deepened the northern basin. The results from gravity modelling improve when the crust is thickened beneath the northern margin of the basin and thinned at the southern margin, as has been suggested by recent deep seismic data. The crustal thickening beneath the basin's northern margin abuts the region of greatest topographic relief and is consistent with the observed structure at the edges of many orogenic belts. If the Officer Basin evolved as a foreland-type basin from the late Proterozoic and has retained those features to the present, then one implication is that in the absence of any significant topography, cratonic lithosphere must be able to support stresses over very long periods of geological time.

INTRODUCTION

A series of E–W-trending Neoproterozoic to early Palaeozoic basins exist within the centre of the Australian plate. They include, amongst others, the Amadeus, Ngalia and Officer basins (Fig. 1) that during their early evolution comprised a single, 2×10^6 km^2 depositional system termed the Centralian Superbasin (Walter *et al.*, 1992). Separating the basins are a series of exposed basement blocks including the Gawler Craton, Musgrave and Arunta blocks. The largest of the present-day intracratonic basins is the Officer Basin, with an area of almost 4×10^5 km^2 (Lindsay & Leven, 1996). As it occupies remote areas of South Australia and Western Australia, where outcrop is limited, its evolution remains poorly understood.

The central Australian region is characterized by an unusual pattern of E–W-trending Bouguer gravity anomalies that are strongly negative over the basins (~ -150 mGal over the Officer Basin), despite the lack of any significant topography (Fig. 2). The gravity field is weakly negative or weakly positive over the basement blocks. These strongly negative Bouguer anomalies are some of the largest observed over the continental interiors (Lambeck, 1983). In addition, the area has not experienced any significant tectonic activity since the Carboniferous ($\sim$ 300 Ma) (Lindsay & Leven, 1996), although erosion of topography has certainly occurred. Thus, it becomes difficult to relate the observed gravity anomalies to present-day tectonism and topography.

The origins of the Officer Basin are obscure and explanations of its initiation are varied, though it exhibits a broadly similar tectonic evolution to the Amadeus and Ngalia basins (Preiss & Forbes, 1981). Previous models have attempted to resolve the complexities of basin evolution in central Australia but have generally

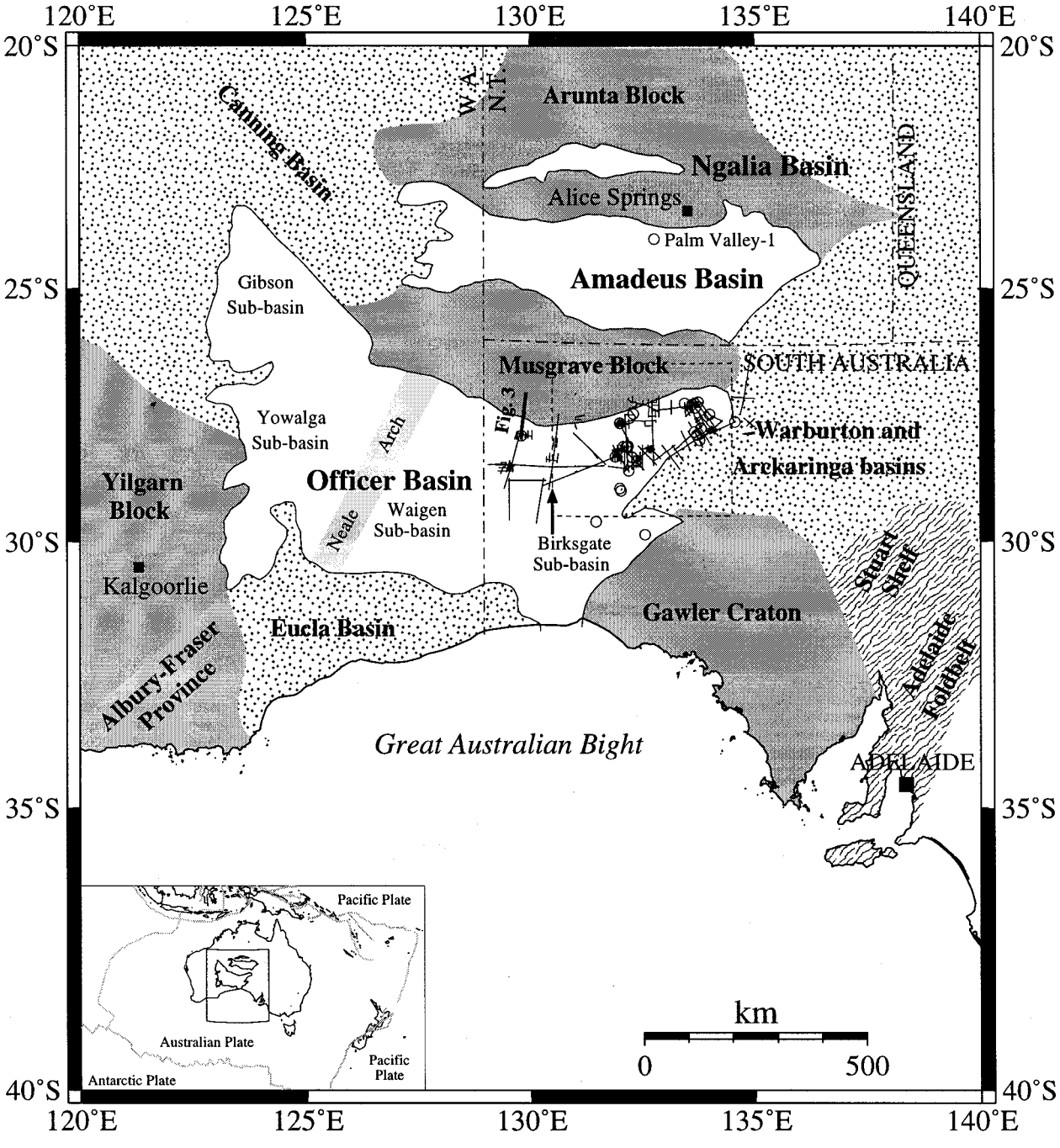

Fig. 1. Location of the Neoproterozoic–Palaeozoic Officer, Amadeus and Ngalia basins in relation to the primary geological provinces. Note the location of the Palm Valley-1 well (Amadeus Basin) that was used as part of the one-dimensional backstripping analysis. The positions of the seismic and well data used to construct the sediment thickness grids are also shown. The grey lines in the inset map represent the main plate boundaries in the region and the dashed black line (inset) shows the position of the 'Capricorn Plate' as inferred by Royer & Gordon (1997).

concentrated on a single tectonic aspect or been limited by a lack of data. Lindsay *et al.* (1987) proposed an extensional cause for the formation of these basins. In the absence of deep crustal data, they studied sediment accumulation curves to determine the modes of basin evolution, concluding that the results were largely indicative of extension. In their model, two extensional phases influenced the region at about 900 and 600 Ma. Both events were thought to have arisen because of the failed rifting of a Proterozoic supercontinent, commonly termed Rodinia (Powell *et al.*, 1994; Wingate *et al.*, 1998; Karlstrom *et al.*, 1999). The observed highstand of sea-level in the Middle Cambrian of the Amadeus Basin (Lindsay, 1987) is also cited as possible evidence for extension and rifting of the supercontinent. A sea-level rise has been inferred on most continents for the Cambrian (Mathews & Cowie, 1979) and has been related to supercontinent breakup (Bond *et al.*, 1984). However,

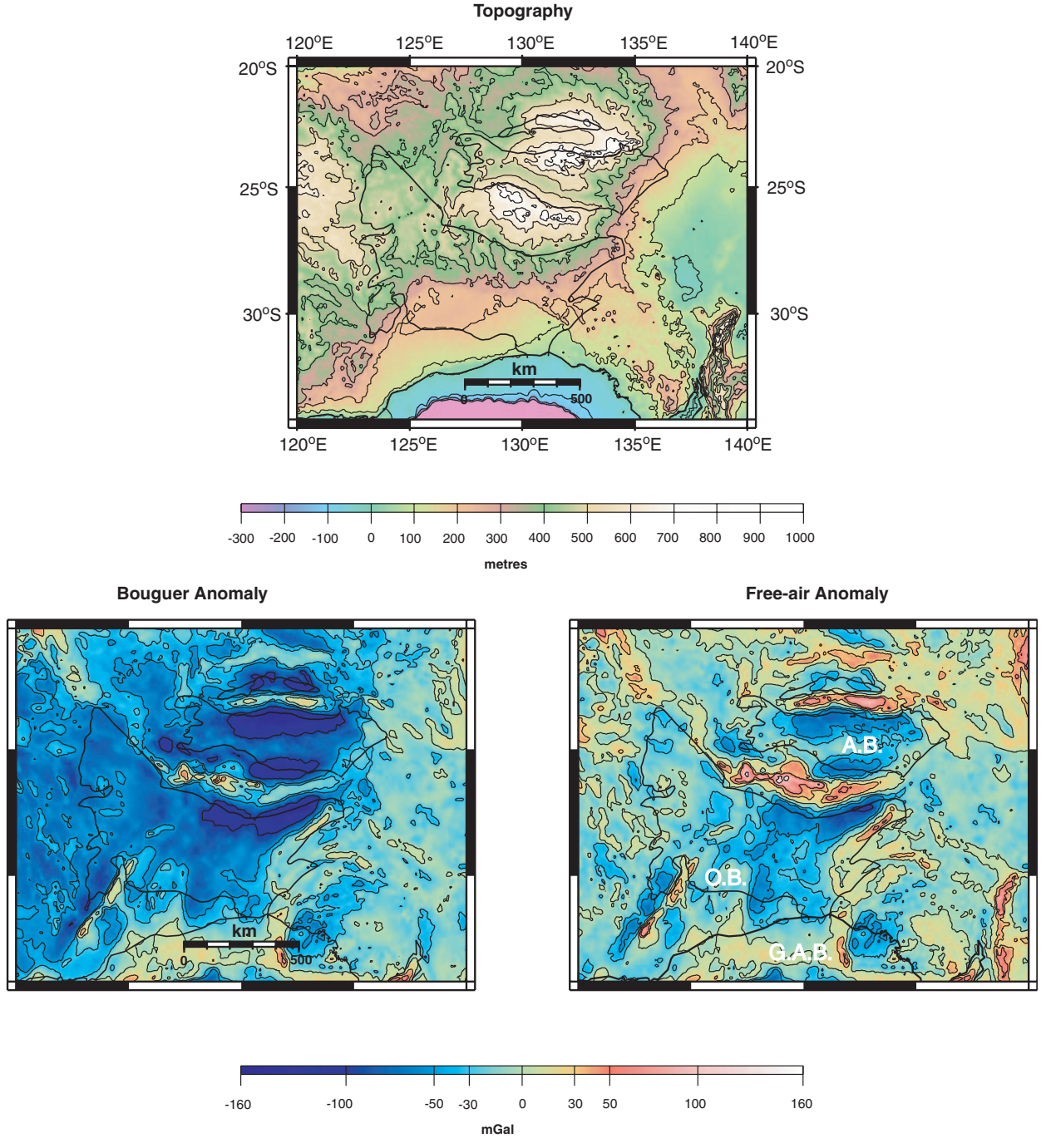

Fig. 2. Topographic (top) and gravity (bottom) maps of the eastern Officer Basin in central Australia. Maximum topographic relief occurs along the northern edge of the Musgrave Block. Locally, Bouguer gravity minima attain amplitudes exceeding − 150 mGal in the northern Officer Basin. OB = Officer Basin; AB = Amadeus Basin; GAB = Great Australian Bight.

Airy models of isostasy predict that rifted crust would also thin, and hence would be associated with gravity highs or near zero anomalies. rather than lows.

Zhao *et al*. (1994) showed that mafic dyke swarms and volcanics from central Australia had uniform geochemical and isotopic signatures over a range of more than 1000 km and interpreted them as the product of a mantle plume. Uplift of the crust would have accompanied mantle upwelling in the Late Proterozoic leading to the formation of a failed rift-arm. Flood-basalt volcanism resulted in some areas and was followed by extension, thinning and thermal subsidence on a large scale, creating an extensive central Australian depocentre (Lindsay, 1999b). Hundreds of metres of shallow marine and fluvial sands were deposited within the Centralian Superbasin, before regional uplift partitioned it into individual basins, at 600–580 Ma (Walter *et al*., 1992; Walter & Gorter, 1994). Likewise, Wingate *et al*. (1998) related dyke swarms to

mantle plume activity, which was considered to be a triggering event for the rifting and breakup of Rodinia.

Comparable extensional and thermal models of basin evolution have also been popular in describing the intracratonic basins of North America, such as the Illinois and Michigan basins, e.g. Green (1983), where the associated gravity anomalies have smaller amplitudes and significant positive components. In these examples, models requiring crustal thinning are far more readily incorporated in studies of the regional gravity field. As a consequence, the classic intracratonic basins of North America may not represent suitable analogues for central Australia.

An alternative to thermal and extensional models for the central Australian basins is a compressional one, as discussed by Lambeck (1983). Having reasoned against graben-type, thermal and foreland-type basin models, he considered the deformation of a viscoelastic plate due mainly to compressional (horizontal or in-plane) forces. The proposed model amplifies the effects of an initial, small, normal load by applying long-term horizontal forces to the plate to produce crustal warping beneath the basin. Although this may explain the observed gravity low, modelling of the gravity field was not conducted by Lambeck (1983). In a similar vein, McQueen & Beaumont (1989) considered models where in-plane compressive stresses resulted in block rotation and the formation of flexural basins. The models produce gravity anomaly lows that correlate with the basins, indicating a lack of local isostatic equilibrium.

The Officer Basin's gravity field was modelled by Mathur (1977). Without the benefit of deep seismic data, he concluded that the near-surface geology accounted for less than a third of the observed anomaly, with the remainder being due to faulting and folding of the crust and upper mantle. Further north, over the Ngalia Basin and Arunta Block, Goleby *et al.* (1989) used a deep seismic reflection line to provide a basis for gravity modelling. Their model also involved thick-skinned deformation, but primarily focused on the Arunta Block and did not target the large gravity lows that are of such interest in the Officer and Amadeus basins.

In light of these ideas and using a compilation of sediment thickness data from the eastern Officer Basin, we attempt to elucidate and refine some aspects of the evolution of the Officer Basin. We adopt a process-orientated approach (e.g. Madon & Watts, 1998), in which combined flexural backstripping and gravity modelling techniques are used to restore the configuration of the crust beneath the basin. In this way, we have been able to test various tectonic scenarios through time and thus processes that may have influenced the basin, such as rifting and orogenic loading. Moreover, because the technique allows for the temporal variation of tectonics and of other parameters such as lithospheric strength, our models are not limited to present-day observations of the crustal structure. Well data from the Officer and Amadeus basins have also been incorporated into the study to examine the timing of tectonic events and determine the pattern of basin subsidence since the Proterozoic.

GEOLOGICAL AND GEOPHYSICAL BACKGROUND

The geological evolution of central Australia is characterized by a long history of metamorphism, plutonism and crustal reworking. The main phase of cratonization of the central continental region occurred at 1300–900 Ma (Plumb, 1979). The existence of a Proterozoic supercontinent and the timing of its breakup has been postulated by Veevers & McElhinny (1976), Piper (1983) and Bond *et al.* (1984) amongst others, and used to explain the early evolution of the Officer Basin (Lindsay *et al.*, 1987).

The Officer Basin forms an elongate, roughly E–W-trending trough that is distinctly asymmetric in N–S profile. The same E–W geometry is observed in the Amadeus and Ngalia basins to the north. The basin may be divided into an eastern and western part separated by the Neale Arch (Hocking *et al.*, 1994), a broad, NE-trending basement ridge (Fig. 1).

The basin's northern margin is a sharp, thrust fault against the Musgrave Block, which has been overthrust to the south (Walter & Gorter, 1994). The Gawler Craton delimits the basin's south-eastern boundary and a number of deep, intervening subbasins are parallel to the margins. Maximum sedimentary thickness is up to 8 km in the western regions of the basin, e.g. the Gibson subbasin (Fig. 1). In the eastern Officer Basin, sedimentary thicknesses are considerably less, being no more than 5–6 km (Walter & Gorter, 1994; Lindsay, 1995, 1999a). To the south, the basin broadens to form a shallow platform that gradually rises from the northern axis.

The history of eastern Officer Basin sedimentation spans ~500 Myr, from initial deposition in the Willouran (~800 Ma) to the latest Carboniferous at about 290 Ma (Moussavi-Harami & Gravestock, 1995) (Fig. 3). Exposure of the sedimentary sequence is poor, due mainly to extensive cover by Pleistocene sand dunes to the north and Quaternary carbonates of the Nullabor Plain to the south. Consequently, much of what is known of the basin's sedimentary architecture comes from limited seismic and well data obtained from mineral and petroleum exploration. A number of 'megasequences' can be identified in the basin. Lindsay & Leven (1996) divide the sedimentary section into six such megasequences (Fig. 3), bounded by regional unconformities.

The earliest megasequence (Willouran) comprises shallow-water sediments that were deposited in an extensive sag basin that stretched from the Kimberley region of NW Australia to the Adelaide Foldbelt in the south-east (Preiss & Forbes, 1981; Walter *et al.*, 1992). This was followed by the Neoproterozoic to earliest Cambrian (~570–550 Ma) Petermann Ranges Orogeny (Lindsay & Leven, 1996; Comacho & McDougall, 2000).

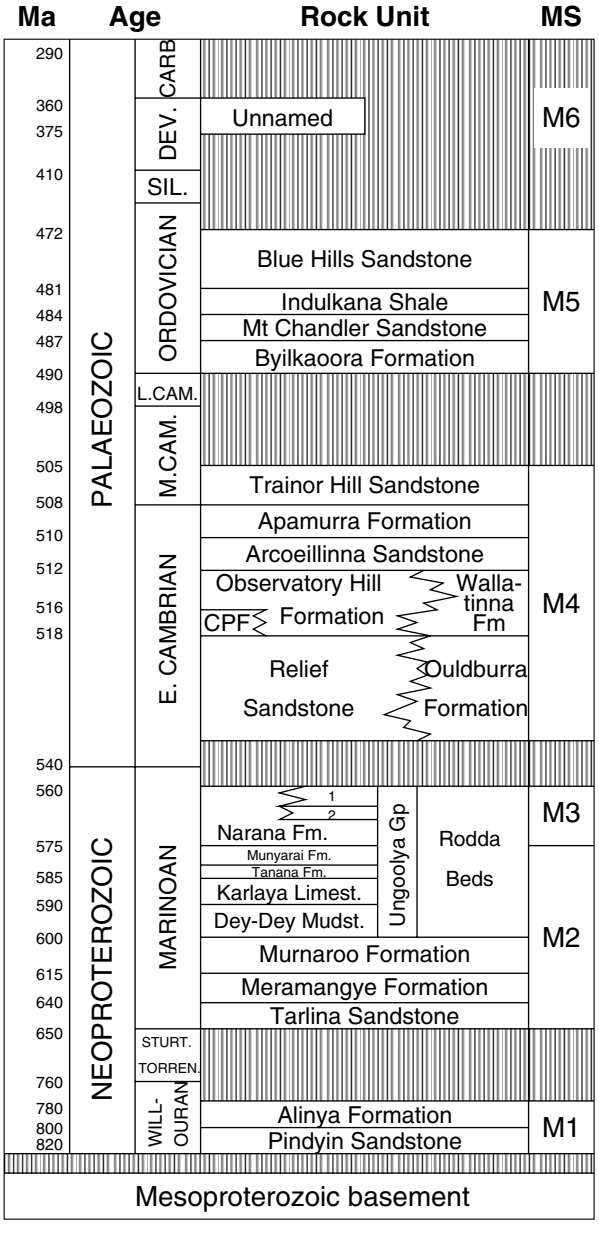

Fig. 3. Generalized stratigraphy for the eastern Officer Basin, based on Moussavi-Harami & Gravestock (1995) and Lindsay & Leven (1996). 1 = Mena Mudstone; 2 = Munta Limestone; CDF = Cadney Park Formation; MS = Megasequence.

K–Ar, ^{40}Ar–^{39}Ar and Rb–Sr data (Comacho & McDougall, 2000) suggest uplift and exhumation of the Musgrave Block had occurred by at least ~550 Ma when thrusts and nappes were produced with accompanying metamorphism (Maboko *et al.*, 1992). A second Cambrian orogenic event, the Delamerian Orogeny, followed and persisted through to the Middle Ordovician. The Alice Springs Orogeny was the final phase of tectonism to affect central Australia, beginning in the Early Devonian (400 Ma) and continuing through to the Carboniferous, at 300 Ma (Cartwright & Buick, 1999; Hand *et al.*, 1999). Intracratonic thrusting and uplift of the bounding cratonic Arunta and Musgrave blocks resulted in the deposition of thick sedimentary sequences in the Amadeus and Ngalia basins (Plumb, 1979), but effectively marked the end of the sedimentary record in the eastern Officer Basin (Fig. 5).

Deep reflection seismic profiles (Lindsay & Leven, 1996; Korsch *et al.*, 1998), teleseismic travel-time studies (Lambeck & Penney, 1984; Lambeck *et al.*, 1988) and seismic refraction data (Wellman, 1982) have revealed information about the deep-crustal structure beneath the central Australian basins and intervening basement blocks. Lindsay & Leven (1996) cite a thickness of approximately 42 km for the crust on which the central Officer Basin rests, a value broadly within the range discussed by Lambeck (1983). Wellman (1982) determined the variation of mean P-wave crustal velocity for continental Australia, deducing crustal thickness values between 37 km and 42 km for the Gawler Craton at the southern edge of the Officer Basin. Most recently, Korsch *et al.* (1998) calculated a depth of 47 km from deep seismic data for the Moho beneath the southern margin of the Amadeus Basin, where it is slightly arched. The Moho beneath the Officer Basin varies from 43 to 48 km depth in the north to 44 km in the south.

Lambeck *et al.* (1988) analysed teleseismic travel-times in terms of an undulating Moho in which the depth varied by as much as 20 km over horizontal distances of less than 50 km. Such a result is consistent with the whole-crustal folding proposed by Lambeck (1983) in modelling the central Australian lithosphere as a viscoelastic plate. Wellman (1982) explained the differences in crustal thickness of the region as arising from lower lithosphere density variations.

Seismic reflection profiles from the area immediately north of the Officer Basin reveal thick-skinned deformation of the crust that has displaced the Moho (Goleby *et al.*, 1989; Korsch *et al.*, 1998). Goleby *et al.* (1989) suggest that the deep structure is primarily responsible for the observed Bouguer gravity field, where thick-skinned thrusting has resulted in significant offsets of the crust/mantle boundary. Lambeck & Penney (1984) distinguished the crust from the mantle on the basis of seismic velocities. They observed that P-wave arrivals were late over sedimentary basins and early over areas of exposed basement. Moreover, late arrivals corresponded to gravity lows and early arrivals to gravity highs, the inference being that the depth to the Moho was highly variable over short distances.

DATA

A total of six megasequences (Lindsay & Leven, 1996) (Fig. 3) were identified and mapped within the eastern Officer Basin from petroleum and mineral exploration data (Fig. 4). This stratigraphy represents the latest evaluation of all seismic (~8100 km) and well data from the South Australian part of the Officer Basin and, unlike some earlier schemes, is based on sequence stratigraphic principles (e.g. Vail *et al.*, 1977). Age control is based on

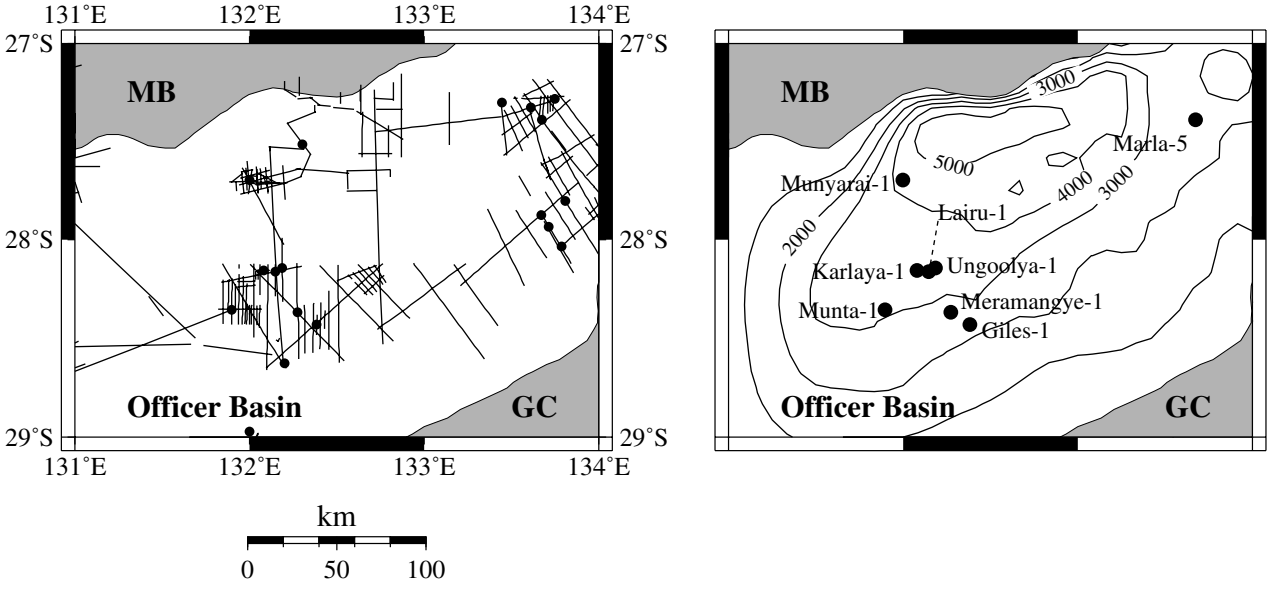

Fig. 4. Outline of the eastern Officer Basin showing the location of seismic and well data used to construct the sediment thickness grids (left) and the cumulative sediment thickness (right). Contour interval is 1000 m. MB = Musgrave Block; GC = Gawler Craton.

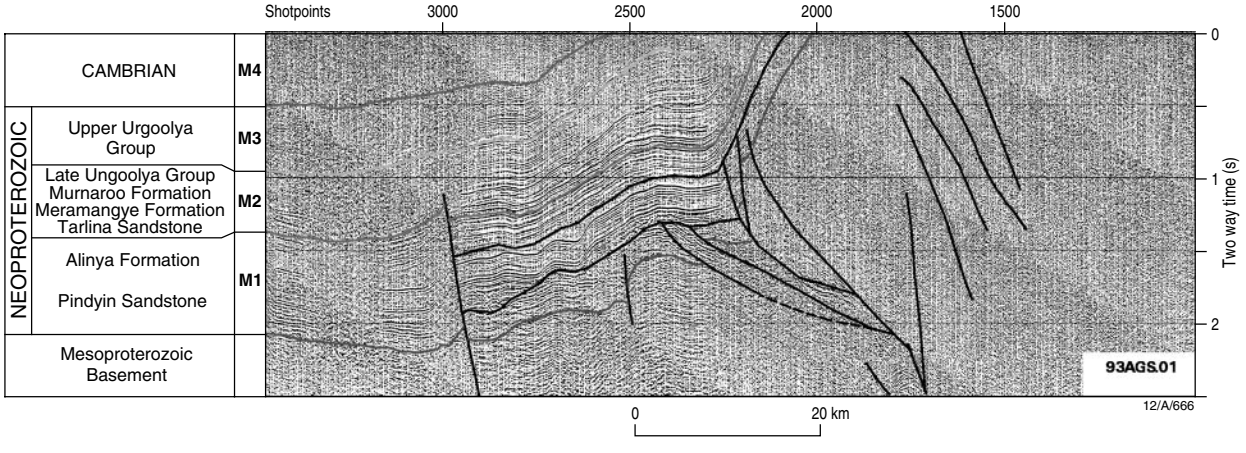

Fig. 5. Two-dimensional seismic reflection line from the Officer Basin with stratigraphy. Location is shown on Fig. 1.

limited palaeontology and radiometric data. The mega-sequences were labelled M1 to M6, from the oldest to youngest sediments (Figs 3 & 5). The resulting isochrons were depth converted using well-log data where possible and RMS velocities where wells were not available. These data were smoothed in $5' \times 5'$ 'bins' then gridded at a $5' \times 5'$ interval using a minimum curvature technique. Zero values of sediment thickness were included in the grid files to correctly taper the sediment thicknesses to where they pinched out. The total sedimentary thickness derived from these data are presented in Fig. 4.

The well data set comprised 26 petroleum and mineral exploration boreholes (Fig. 4). Of this number, eight wells from the Officer Basin contained a sufficiently long sedimentary record for 1-D backstripping analysis. One well from the Amadeus Basin was included for comparative purposes. In addition, sonic data from the wells were digitized, converted to porosity and the resultant data fitted to a soil mechanics compaction profile (Audet, 1995), using a least squares method. It has been shown (Baldwin & Butler, 1985) that traditional methods of deriving compaction profiles, e.g. Athy (1930), underestimate the surface porosity of sediments and the use of alternative methods of compaction analysis is warranted. Furthermore, the soil mechanics approach is based on the observable compaction behaviour of sediments.

The gravity data used in this study were compiled by GETECH as part of its Southeast Asia Gravity Project, which provided smoothed Bouguer values (onshore) at a $5' \times 5'$ spacing. These points were then gridded at the same interval for use in the models.

SUBSIDENCE HISTORY

One-dimensional backstripping

In order to address the problem of the origins of the Officer Basin, a simple one-dimensional backstripping analysis was conducted. Tectonic subsidence curves deduced from backstripping help to differentiate between extensional and compressional events and to show their relative timing. For the purposes of comparison and to test the possibility that the central Australian basins were formed simultaneously by a continent-wide mechanism such as whole-crust warping (Lambeck, 1983), a similar analysis was conducted for a well in the Amadeus Basin, approximately 300 km to the north. The Officer Basin wells extend from the shallow, ramp-like southern margin of the basin, to its deep, thrust-controlled northern margin (Fig. 6). Palaeobathymetric corrections were not considered for the Officer Basin as it is believed to have been a shallow-water or subaerial depocentre (Gravestock & Hibburt, 1991; Sukanta, 1993; Lindsay & Leven, 1996). Neither was a sea-level correction applied because of uncertainties in global sea-level during the Proterozoic.

Two features are common to all wells: the small amount of total tectonic subsidence for their longevity (generally <1000 m) and the long hiatus in the sedimentary record (post 500–450 Ma) which prevents the recovery of subsidence data (Fig. 7). Most wells display early and rapid subsidence from 650 to 450 Ma although the magnitude is small at Marla-5 and Meramangye-1. The Marla-5 curve is particularly featureless, though this may be a function of the amount of section penetrated in the well.

This early subsidence event shows evidence of progressively increasing subsidence rate which is best seen at Karlaya-1, Lairu-1, Munta-1 and Ungoolya-1. Such a pattern of subsidence is typical of foreland basins, where the encroaching orogenic mass progressively loads the lithosphere (e.g. Haddad & Watts, 1999). This is particularly evident at Munta-1, but the effect is more subtle at Karlaya-1 and Lairu-1. A period of 40 Myr of erosion or nondeposition commencing at 560 Ma terminates the first phase and marks the beginning of the second, where the increasing rate of subsidence is more readily observed than in the first phase. All four wells display this feature. The termination of this second phase generally marks the beginning of the long hiatus in the sedimentary record of the eastern Officer Basin.

The exception to this pattern is Munyarai-1. Total tectonic subsidence exceeds 1000 m and continues beyond the times observed in all other wells, albeit at a lower rate. The early tectonic subsidence resembles that seen in other wells. Where the others exhibit a second short phase of subsidence, Munyarai-1 displays an almost uninterrupted period of tectonic subsidence lasting approximately 200 Myr from 575 Ma, or about 100 Myr longer than any other well. The Munyarai subsidence appears to be a function of its location in the northern Officer Basin, suggesting that it was affected by the Alice Springs Orogeny that deformed the Amadeus Basin.

The first two phases, from 650 to 560 Ma and 550 to 450 Ma, are broadly correlative with the Petermann Ranges (or younger) and Delamerian orogenies (Fig. 7). According to Lindsay & Leven (1996), the Petermann Ranges Orogeny was a short-lived and relatively localized episode lasting for 15 Myr from 575 Ma. At Lairu-1, Ungoolya-1, Karlaya-1 and Munyarai-1, the earliest parts of the subsidence curves appear closely related to this event, with the remaining wells apparently less affected by the tectonism. The Delamerian Orogeny (505–472 Ma) correlates well with the second phase subsidence. This is observed at Karlaya-1, Lairu-1, Munta-1 and Ungoolya-1 and matches increased rates at Munyarai-l.

The early period of tectonic subsidence is succeeded in all cases by a long hiatus representing nondeposition or erosion, as signified by the long, flat part of the curves. With the exception of Munyarai-1, subsidence cannot be recovered from 450 Ma to the present, as in general, rocks no younger than Carboniferous age form the uppermost part of the eastern Officer Basin sedimentary section.

Only one well from the Amadeus Basin, the Palm Valley-1 well, was available for analysis (Figs 1 & 7). The rocks encountered in this well range in age from the Late Cambrian to Early Carboniferous. Most of the observed tectonic subsidence at Palm Valley-1 took place in the period 490–435 Ma (Fig. 7). Early subsidence gave way to a period of approximately 65 Myr of nondeposition or erosion. The last major subsidence event began at 375 Ma, occurring in two parts: 170 m of subsidence over 10 Myr and; 85 m over the next 65 Myr.

The earliest period of subsidence appears to be related to the Delamerian Orogeny. Older stratigraphic data were not available to determine the origin or extent of early subsidence. The second major pulse, however, occurred during the Alice Springs Orogeny (400–300 Ma) (Fig. 7) and so may be related to this tectonic event.

The Amadeus Basin curve shows some broad similarities with Officer Basin wells. Both basins begin with early, sharp subsidence episodes, both are interrupted by 40–60-Myr periods of erosion or nondeposition and the tectonic subsidence in both basins is eventually dominated by a long hiatus in the sedimentary record. Although the subsidence patterns are broadly similar in the two basins, an important difference arises. Except in the case of Munyarai-1, significant subsidence in the Amadeus Basin continues for 130 Myr beyond the time that erosion or nondeposition dominate the eastern Officer Basin. Despite Palm Valley-1 only representing a portion of the ages encountered in Officer Basin wells, it appears that the eastern Officer Basin was affected to a lesser degree by the tectonics driving the main subsidence episode at Palm Valley-1.

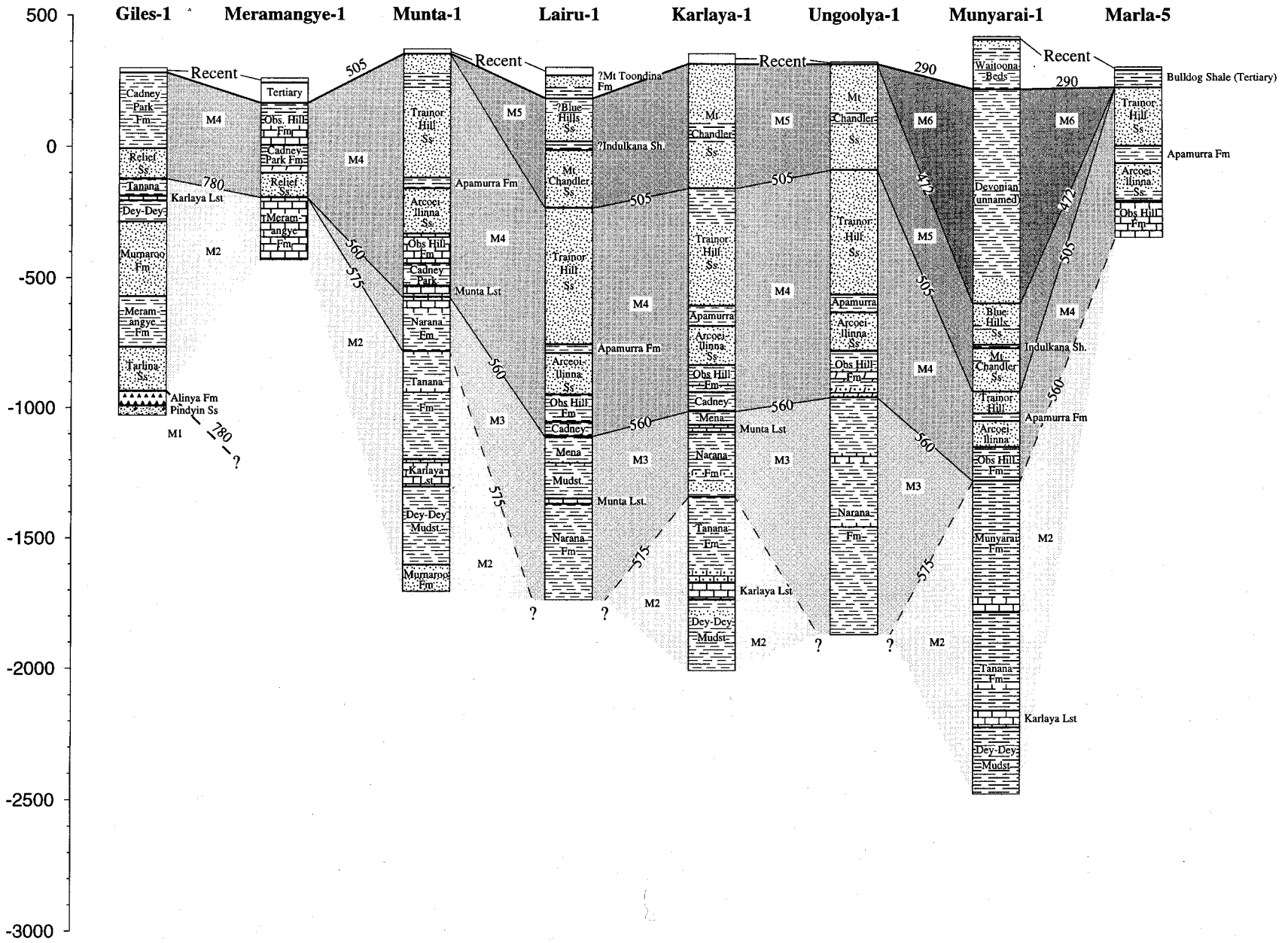

Fig. 6. Well sections for the eight eastern Officer Basin wells used in 1-D backstripping. Giles-1 is located towards the southern basin margin and Munyarai-1 near the northern margin. Marla-5 is located in the most easterly part of the basin. The six megasequences are identified, labelled M1 to M6, and the age of their boundaries is also shown.

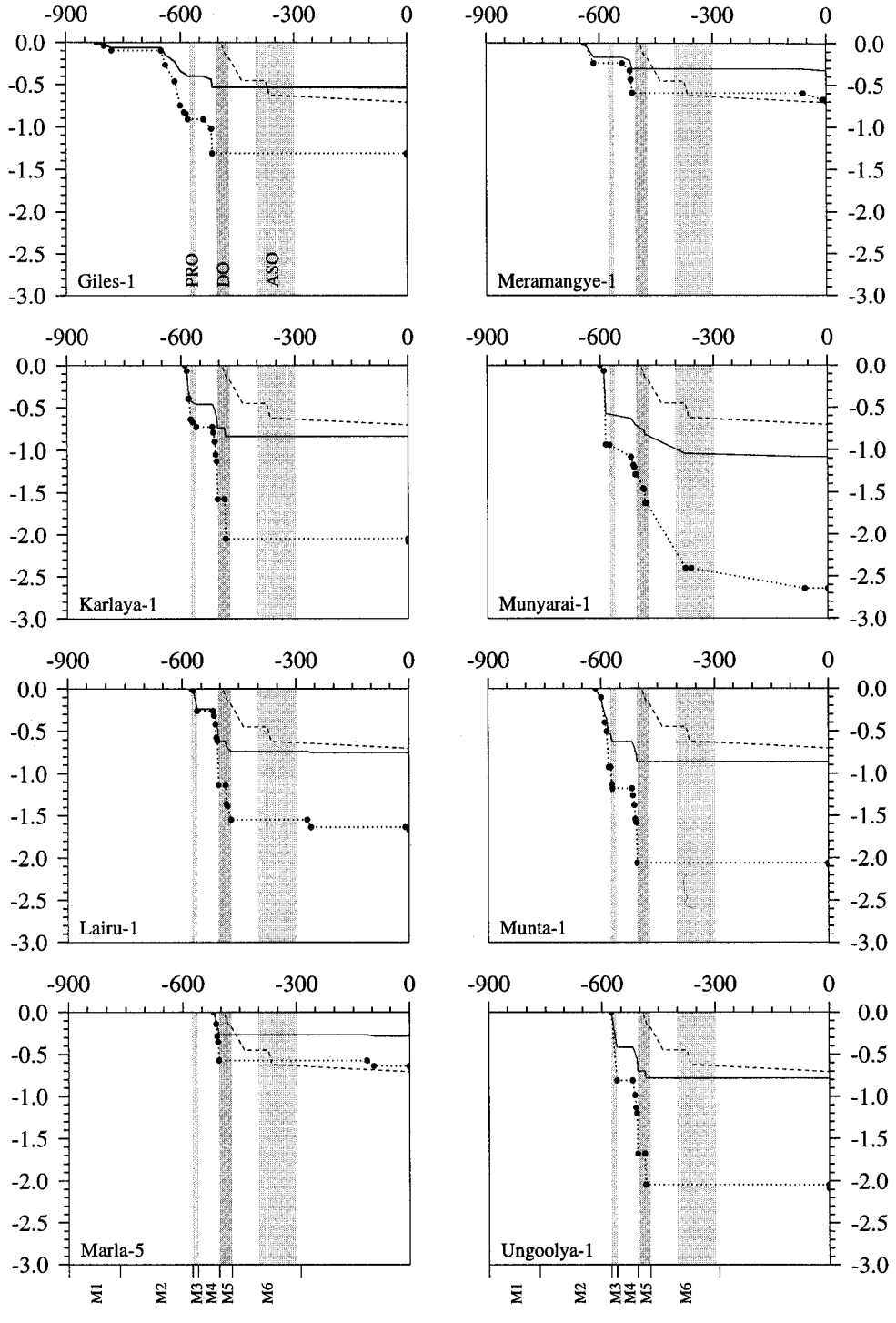

Fig. 7. A comparison of one-dimensional backstripping results from central Australia (solid lines). Each box represents a tectonic subsidence curve for an eastern Officer Basin well. In all cases, the dashed subsidence curve is that of the Palm Valley-1 well, situated in the Amadeus Basin to the north. The dotted lines represent the observed sediment thickness at each well and the dots show the stratigraphic control points. The grey strips indicate the timing of the main orogenic events to affect central Australia according to Lindsay & Leven (1996). PRO = Petermann Ranges Orogeny; DO = Delamerian Orogeny; ASO = Alice Springs Orogeny.

Three-dimensional flexural backstripping

The backstripping method used to calculate the curves shown in Fig. 7 is based on the assumption of Airy isostasy. Hence they do not take flexure into account. In order to investigate the role of flexure, the basement was unloaded using different assumptions about the flexural strength of the underlying lithosphere.

Flexural backstripping (e.g. Watts, 1988) involves the progressive unloading of stratigraphic sequences through time. In the case of the Officer Basin, flexural unloading of the lithosphere removed six sedimentary megasequences

(Lindsay & Leven, 1996), using a three-dimensional technique that employs an FFT routine to calculate the preloaded basement profile. Each megasequence was represented by a $5' \times 5'$ grid of sedimentary thickness, determined from well and seismic data. Megasequences M5 and M6 were treated as a single unit because they are structurally concordant and sedimentologically similar. Mantle density was assumed to be 3330 kg m^{-3} and the average crustal density to be 2800 kg m^{-3}. Based on seismic velocities, fully compacted sediment densities used in the models ranged from 2400 to 2720 kg m^{-3}. As flexural backstripping results are dependent on T_e, the basement was backstripped for three cases: a uniformly strong plate (i.e. high T_e); a uniformly weak plate (i.e. low T_e); and a plate where strength depends on the age of the plate at the time of loading. Low T_e models follow the assumption that continents are weak and remain weak for long periods following extension (e.g. Watts, 1988). High T_e models of the continental lithosphere are proposed by Bechtel *et al.* (1990) and Zuber *et al.* (1989) which suggest that stable cratons are capable of considerable strength ($T_e > 80$ km for the interior of the Australian continent). A third model (e.g. Karner *et al.*, 1983) aimed to incorporate elements of the previous two cases, so that strength increases with the age of the lithosphere. Following a heating event at the time of basin initiation, the lithosphere was allowed to regain its strength over time, according to observations from the oceans, where $T_e = 3\sqrt{t}$, and t is the time since rifting. It has been shown for the oceanic lithosphere (e.g. Watts, 1978) that the strength can be approximated by the depth to the 450 °C isotherm. However, it is not clear if continental T_e is controlled by a similar isotherm (e.g. Burov & Diament, 1995; Lowry & Smith, 1995).

When $T_e = 0$, only subsidence (no positive topography) is recorded in the basin (Fig. 8A). Tectonic subsidence accounts for a maximum of 2600 m, or 40% of the observed (present-day) basement depth. When T_e is very high, then most observed subsidence is tectonic and the sediment load has little local effect (Fig. 8B). When

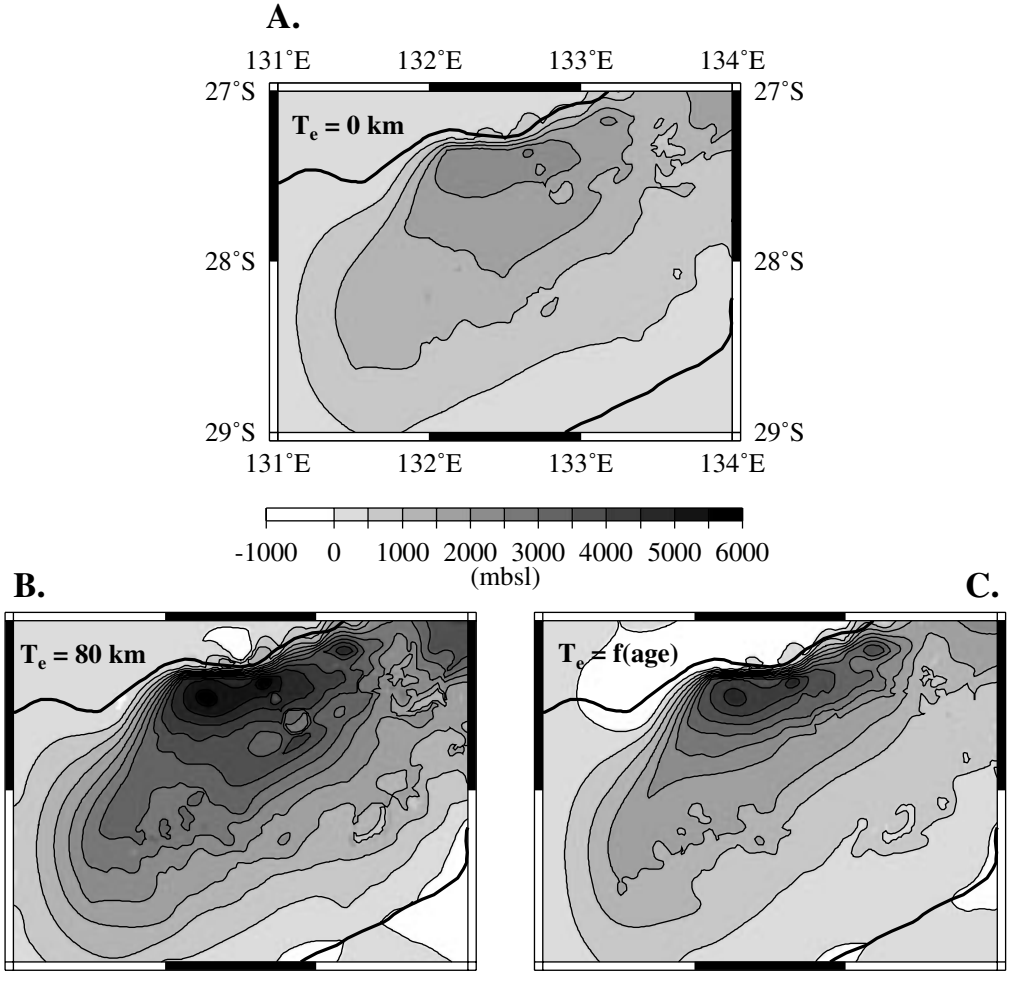

Fig. 8. Backstripped position of the basement in the eastern Officer Basin for different T_e to the end of M6-time. Sediment-enhanced subsidence is greatest when $T_e = 0$ (A). When T_e is high (B), sediment loading has little influence on basement depth. When T_e is a function of age, the resulting backstripped basement is more asymmetric in the north–south direction than for time-invariant T_e (C) and the deeper parts of the depocentre are more areally restricted and elongate. Contour interval is 500 m. See Fig. 4 for data location.

$T_e = 80$ km, tectonic subsidence accounts for over 90% of the observed basement depth. When T_e varies over time (Fig. 8C), changes in both the depth and the shape of the basin occur. Elastic thickness did not exceed 45 km in the modelled case of time-dependent T_e, yet the tectonic subsidence still accounted for a maximum of 75% of the observed.

An important difference between basement that is corrected for sediment loading using high T_e and low T_e is the positive topography (i.e. elevation above sea-level) created at the edges of the loads. Figure 8(B,C) clearly show when T_e is not zero, positive topography is restored to the basin's flanks. The magnitude and wavelength of this elevation are dependent on plate strength and the distribution of the sediment load.

Basin margin flexural uplift is also well illustrated by Fig. 9 which shows the results from flexurally back-stripping individual megasequences and represents the amount of tectonic subsidence for each megasequence. Figure 9 compares the normalized subsidence of weak, strong and variable T_e lithosphere (0–80 km) and emphasizes that both the amplitude and the wavelength effects of the variation. When $T_e = 0$, no positive topography is restored. When T_e is set to 80 km, the height of the elevated areas is subdued, but there is a dramatic broadening of subsidence patterns over the basin.

The influence of the individual tectonic subsidence events on the overall tectonic subsidence history is also highlighted by Fig. 9, which demonstrates the variation of geometry and locus of subsidence through time. At a time corresponding to M1, subsidence is diffuse and several maxima are visible across the basin. In contrast, M2-time sees a roughly triangular pattern established along the northern margin of the basin with the maximum located at the apex. A diffuse subsidence pattern again developed in M3-time, where the maxima are more isolated when T_e is low. Most of the restored positive relief occurs at the basin edges during M2- and M3-time, though it is more prevalent in the latter. An elongate subsidence pattern characterizes M4-time and is located towards the centre of the basin. It parallels the basin margins and shows a second area of subsidence developed in the north-eastern corner. Positive areas occur mostly at the northern margin. The final megasequence is dominated by elliptical patterns for all cases. Positive relief is widespread and, in the cases of higher T_e, isolates the main area of subsidence against the northern margin of the basin. Subsidence is therefore dominated by linear trends that are centred near, and parallel to, the northern margin, the wavelength of which is governed by T_e.

FLEXURE AND GRAVITY MODELLING

The age of the Officer Basin and its long isolation from active plate boundaries have resulted in subdued topography, where the maximum elevation of the region is less than 1000 m. Topography in central Australia is generally in the range of 100–900 m (Fig. 2A) with a decrease of elevation towards the southern Officer Basin. On the other hand, the Bouguer gravity field is unusual for a continental interior. The region is dominated by the intensity of the negative anomalies (Fig. 2B,C), which are difficult to relate to flexural models of the lithosphere, assuming only surface topographic loading. Within the eastern Officer Basin, the Bouguer anomaly is asymmetric. The most negative anomalies occur along the north-eastern margin of the basin, adjacent to the Musgrave Block. In general, positive Bouguer gravity anomalies are resticted to the shorter wavelengths of the field and mostly correspond to the cratonic blocks bounding the basin.

Two-dimensional gravity modelling

In an attempt to constrain the processes that have modified the basin through time, a 'process-oriented' approach to gravity modelling was adopted. In this approach (e.g. Madon & Watts, 1998), certain assumptions are made about the state of the crust (e.g. thinned or warped), the gravity effects of which are then tested against observations. The models were designed to simulate a rift-type basin, an uncompensated basin and a foreland-type basin.

The first model (Fig. 10A) considered a rift-type basin as postulated by Lindsay *et al*. (1987). The normal crustal thickness was set to 42 km (Lindsay & Leven, 1996) and is broadly in line with estimates of crustal thickness based on seismic reflection data (e.g. Korsch *et al*., 1998). The rifted crustal geometry was calculated by backstripping the basin in three-dimensions to restore the basement to a presedimentation profile, which was assumed to have been created by lithospheric stretching. The compensation for the basin was then computed from this restored profile using Airy compensation of a single layer crust.

In this simple, first model, the basin fill was assumed to be a single depositional unit, i.e. no distinction was made between the densities of the megasequences. The 'rifting anomaly' is calculated without any sediment in the basin and is a composite of the negative gravity anomaly arising from the water-filled depocentre and the positive anomaly created by the thinning of the crust (Fig. 10A). Adding a sediment load acts to flex the lithosphere to a deeper profile, the magnitude of which is dependent on T_e. The resulting 'sedimentation anomaly' is a positive anomaly with flanking lows. The addition of the component anomalies produces the sum gravity anomaly for the basin, which may then be compared to the observed.

The positive, 'final anomaly' produced by a rift-type basin does not replicate the observed gravity anomaly (Fig. 10a). Rift basins should produce positive anomalies or anomalies that oscillate about zero magnitude as the upwelling mantle acts to compensate the negative effects of basin formation. However, the rift-type model could not reproduce the negative anomalies required for the eastern Officer Basin, irrespective of the T_e used in the calculations.

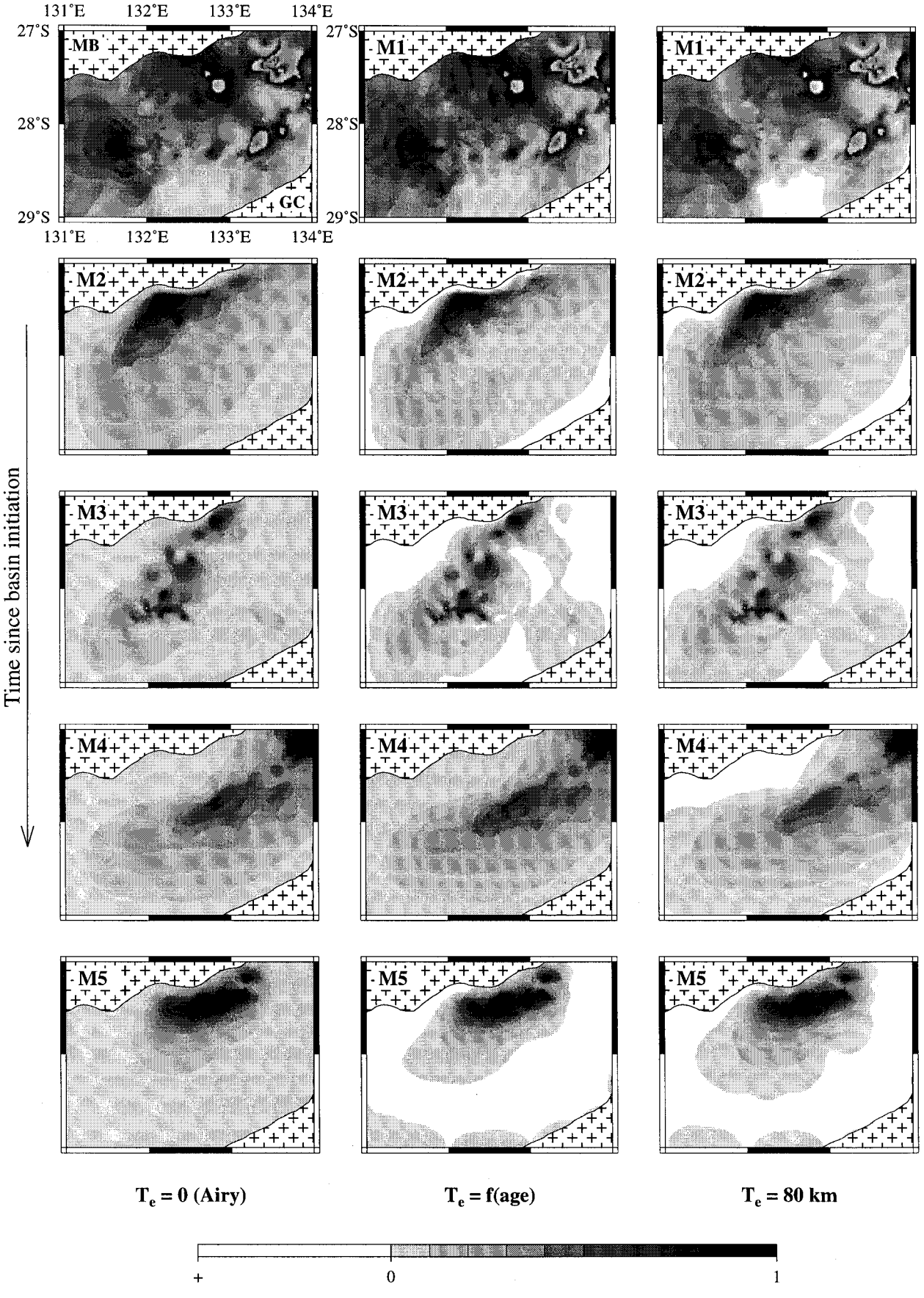

Fig. 9. Normalized subsidence results for the Airy compensation, high T_e and strength variation with age. The areas of positive relief (white regions) are generally broader in the case of varying T_e with age. MB = Musgrave Block; GC = Gawler Craton; M1–M5 = megasequences M1 to M5.

An alternative mode of basin support involves the concept of an undercompensated or uncompensated depocentre (Fig. 10B), in which the root is either of reduced dimension or not present beneath the basin (e.g. Madon & Watts, 1998). Such a model could arise from strike-slip faulting, where faults juxtapose crustal blocks of different thickness. The principal effect of reduced isostatic compensation is to enhance the negative amplitude of the final anomaly. When compared to the total, a better fit to the observed data can be seen than for the rift model. In effect, the crust has been thickened beneath the basin, adding a mass deficit that generates a negative anomaly (Fig. 10B).

In the third case (Fig. 10C), a foreland-type model, the crust was assumed to flex in response to an external load, such as a thrust and fold load. The crust/mantle interface is significantly depressed, creating a large mass of anomalously low density at the base of the crust, constituting a northward deepening of the Moho towards the Musgrave Block. Recent deep seismic reflection studies (Korsch *et al*., 1998) indicate that the Moho depth increases towards the north, from 43 km to 48 km. In Fig. 10(C), it was assumed that the amount of flexure at the crust–mantle interface was equivalent to that at the surface. This further enhances the negative amplitude of the final anomaly and produces the best overall fit of the three basin types (Fig. 10). The misfit between the anomalies becomes more pronounced at the extremities of the profile. However, their wavelengths (up to $\lambda = 100$ km) are in broad agreement and the peak magnitudes are comparable.

Three-dimensional gravity modelling

The sediment thickness grids used to backstrip the basin and restore the basement to its preloaded position can also be used to model the basin's gravity field in three dimensions. By using the same philosophy adopted for the two-dimensional case, a process-orientated forward model can be applied across the eastern Officer Basin to investigate the processes that may have influenced the region.

Figure 11 illustrates the three-dimensional gravity model results, based on the foreland-type basin model. The model initially assumed a uniform thickness crust of 42 km and was tested for T_e of 5–80 km with the component densities (sediment, crust and mantle) the same as those previously used. Figure 11(A) also shows the observed Bouguer anomaly field with the basin's main faults. The NE–SW fault orientations are mirrored by the trend of the observed field. The gravity anomalies are largely negative, particularly towards the Birksgate Sub-basin, though a linear and weakly positive anomaly correlates with the fault patterns. This positive anomaly occurs near prominent basement structures like the Ammaroodinna Ridge.

The calculated gravity field based on the backstripped tectonic subsidence (Fig. 11B) reproduces much of the negative field observed in Fig. 11(A). Although there is a gentle, SE-directed decrease in the magnitude of the negative anomaly, positive values are never obtained by the model. The negative magnitude of the calculated anomaly attains the correct peak values of the observed gravity data but the minima are not coincident. To the north-west, the calculated profile is much more positive than the observed, while to the south-east, the opposite is true. This is illustrated by the residual gravity field, plotted in Fig. 11(C). Its most obvious feature is the broad, intense, ridge-like high trending NE–SW, indicating the positive excess of the observed field over the calculated. The residual high is closely correlated with the fault structure and basement topography. In fact, the faults are almost entirely restricted to this residual high, and coupled with its comparatively short wavelength, suggests a possible control of basement (shallow) structure on the observed field. To the north-west, the residual field indicates that the calculated anomaly cannot predict the negative magnitude of the observed field for the given crustal model. However, the shape and wavelength of the observed and calculated anomalies in profile (Fig. 11D) are not markedly different, despite the poor fit between the two towards the edges.

In order to better explain the residual gravity anomalies and improve the model results, the assumption of a constant thickness crust was reconsidered. Large variations in the depth of the Moho have been suggested by Lambeck & Penney (1984), Goleby *et al*. (1989) and Lambeck *et al*. (1988) amongst others, based on evidence from seismic data. Therefore, a foreland-type model of the crust was thickened towards the northern margin of the basin and thinned to the south. The resulting gravity anomalies reflect the equivalent amount of crustal thickening or thinning required to fit the observed and calculated fields.

Figure 12 shows the gravity modelling results and the deep crustal structure that is required to produce them. The geometry of the Moho for a preloaded crust is shown in Fig. 12(e). The south-eastern half of the basin is dominated by a ridge of mantle material that correlates with the mapped fault patterns. The maximum amount of thinning is 8.3 km from the regional average of 42 km, placing the mantle at a minimum depth below the surface of 33.7 km. To the west and north-west, the crust is thickened by up to 12 km so that the base of the crust is at a maximum of 54 km depth. This geometry is reflected in Fig. 12(F), and is a representation of the crustal thickness beneath the eastern Officer Basin. It is evident that much of the crust is now less than 42 km thick, although the flexural influence on the basin has been taken into account.

The calculated gravity (Fig. 12B) now more closely resembles the observed. Although it still lacks the elongate high of the observed field, the calculated gravity is more positive towards the south-east (Fig. 13). The misfits are of reduced amplitude and wavelength, although fault locations still correspond to the areas of

least agreement. Therefore, we propose a model that would satisfy the observed gravity data (Fig. 13). It is possible to envisage a scheme in which a variable thickness crust is subjected to orogenic loading, resulting in crust thickened towards the thrust belt at the basin's northern margin to produce large, negative gravity anomalies.

DISCUSSION

The longevity of intracratonic basins naturally exposes them to multiple tectonic episodes and modifying processes like erosion, which causes them to develop complex histories. However, the Officer Basin tectonic subsidence curves show only a small cumulative

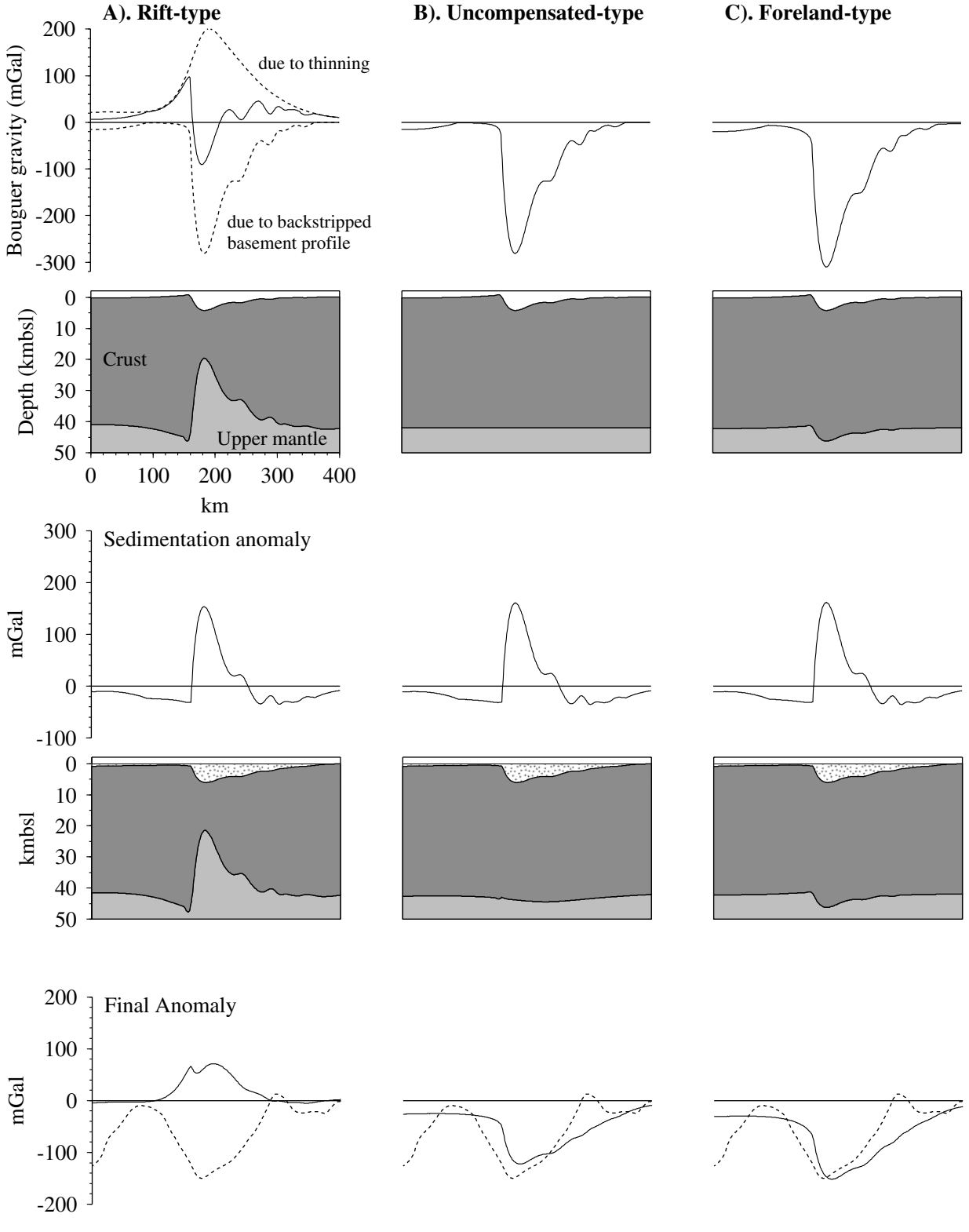

subsidence, primarily reflecting the early tectonic history of the basin. Both the one-dimensional subsidence curves and three-dimensional models reveal a basin with a seemingly dominant, early period of tectonism (i.e. M2-time) that influences later development.

The origins of the Officer Basin remain enigmatic as both the one-dimensional and three-dimensional cases are affected by the gap in the sedimentary record that follows the deposition of megasequence M1. A rift cause for basin initiation (Lindsay *et al*., 1987) is unlikely given that the whole of central Australia (some 2×10^6 km^2), was a single depositional system at M1-time (Preiss & Forbes, 1981; Walter *et al*., 1994, 1995). The mantle plume hypothesis of Zhao & McCulloch (1993) and Zhao *et al*. (1994) remains a possibility as it provides a mechanism that can explain the dimensions of the Centralian Superbasin. Furthermore, Lindsay (1999b) claims that the basal sandstones within the Amadeus Basin and their correlatives in other central Australian basins are related to mantle plume activity as they were all once part of a vast, sheet-like, quartzose sand that was deposited as most of central Australia formed a shallow regional depocentre.

DeRito *et al*. (1983) considered the mechanisms that drive subsidence in cratonic basins. They envisaged a model whereby subsidence from a continental rift event was periodically reactivated, perhaps as a result of compressional tectonics. Based on a viscoelastic plate model, the subsidence was calculated to cease only when isostatic compensation is achieved. That significant tectonic subsidence has ceased in central Australia is almost certainly the case. The reactivated periods of subsidence described by DeRito *et al*. (1983) are related to horizontal regional stresses. However, the one-dimensional backstripping results from central Australia generally show no evidence for reactivation of subsidence in the last 300 Myr, despite it being proposed that considerable intraplate stresses exist elsewhere in the Indo-Australian Plate (Weissel *et al*., 1980; McAdoo & Sandwell, 1985; Cloetingh & Wortel, 1986; Zoback *et al*., 1993). Moreover, both the Bouguer and the free-air gravity maps for central Australia (Fig. 2) exhibit strongly negative anomalies, which suggests that the region is not in isostatic equilibrium.

In a similar vein, Lambeck (1983), Stephenson & Lambeck (1985) and Shaw *et al*. (1991) invoked in-plane stresses acting on the whole of central Australia to produce a series of east–west-trending basins. The tilting block model of basin formation (McQueen & Beaumont, 1989) can also explain the formation of the central Australian basins as well as the apparent isostatic disequilibrium. However, in the light of the backstripping results presented here, whole crustal warping or block tilting as the primary tectonic mechanism remains contentious because it implies simultaneous deformation across the region, which is at odds with the comparisons between Officer and Amadeus basin wells. The one-dimensional subsidence plots suggest that the bulk of subsidence magnitude in the Officer and Amadeus basins were not coeval. Later, Amadeus Basin deformational events apparently had a more limited effect (although local effects may have been considerable) on the eastern Officer Basin than earlier tectonism.

The accelerating subsidence observed at many foreland-type basins is also seen in the Officer Basin. Orogenic activity in the basin is well documented (e.g. Lindsay & Korsch, 1989; Shaw *et al*., 1991) and is particularly reflected at time-M2 (650–580 Ma). Slow subsidence and nondeposition are succeeded by rapid, and in some cases by accelerating rates. Increased subsidence in the north-west is probably related to the proximity of wells to the thrust mass and the extent of thrust advancement. A foreland-type model had been previously dismissed because the basin is not presently located near a plate boundary (Lambeck, 1983). However, the results of this study would seem to indicate foreland-type evolution where deformation is driven by thrusting of cratonic blocks. Other studies have proposed the existence of foreland basins in continental interiors, such as the Kilohigok Basin ($\sim$ 1.9 Ga old) in the Slave craton of Canada (Grotzinger & Royden, 1990).

The Officer Basin's long history of tectonic quiescence, coupled with apparent isostatic disequilibrium under the influence of compressive in-plane stresses, argues for a lithosphere that can support and maintain stresses over very long periods of time, as was suggested by Beekman *et al*. (1997). The rapid subsidence that can accompany faulting in extension (Dewey, 1982) is also an unlikely cause for the observed rates of subsidence, since time M1 is a known period of compressive tectonism,

Fig. 10. The process-orientated modelling scheme illustrating the effects for three different modes of basin formation. In each model, the tectonic subsidence (and uplift) deduced from flexural backstripping has been used to restore the crustal structure. (A) A rift-type basin in which the Moho configuration has been computed from the backstrip assuming Airy isostasy. The uppermost gravity anomaly shows the individual contributions (dashed lines) to the so-called (e.g. Watts, 1988) 'rifting anomaly' (solid line), which is the gravity effect associated with the thinning of the crust at the time of rifting. The middle anomaly profile shows the 'sedimentation anomaly' due to sediment loading and its (flexural) compensation. The lowermost profile shows the 'final anomaly' which displays a distinctly positive gravity anomaly (solid line) that is at odds with the deeply negative observed Bouguer anomaly (dashed line). (B) An uncompensated basin that may be produced by a large strike-slip fault system. The modelled 'final anomaly' is now strongly negative like the observed Bouguer anomaly. (C) A foreland-type basin produced by elastic bending. This model results in the closest fit between the observed and calculated Bouguer gravity anomalies as crustal thickness is preserved. The resulting synthetic anomaly is now equal in negative amplitude to the observed Bouguer anomaly with good wavelength fits up to $\lambda = 100$ km.

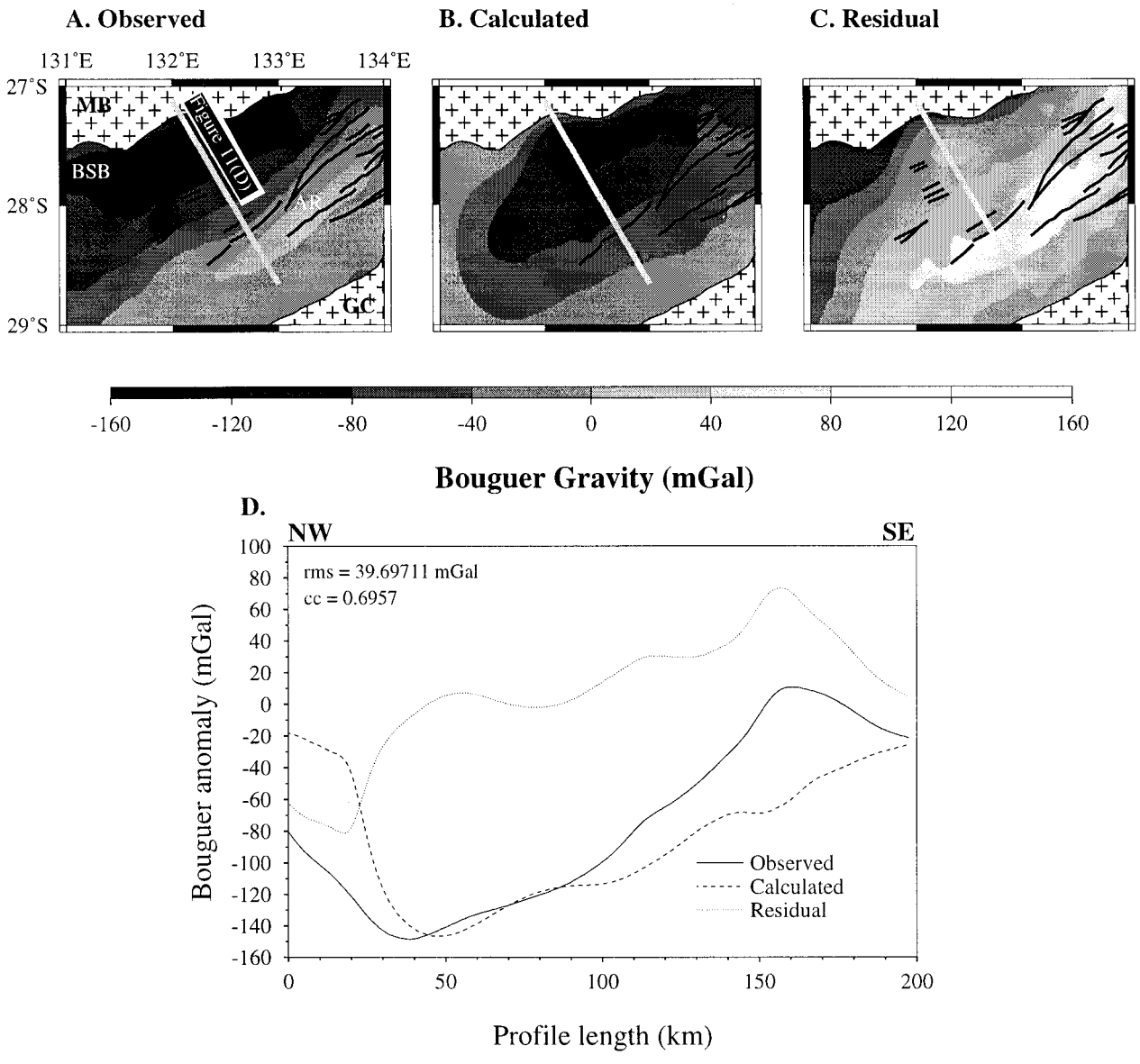

Fig. 11. Results from three-dimensional, process-orientated gravity modelling. The positions of the major faults are shown on all figures. Note the correlation between the positions of the positive residual anomaly (observed – calculated) and the shallow faulting. The straight line represents the location of the sample profile shown above (D). The overall shape and maximum negative magnitude of the calculated profile are in general agreement with the observed, though the obvious difference in gradients is reflected in the root mean square fit (rms) and correlation coefficient (cc). MB = Musgrave Block; GC = Gawler Craton; BSB = Birksgate Sub-basin; AR Ammaroodinna Ridge.

reverse and thrust faulting being evident in seismic data (Fig. 5).

Other evidence points to the basin's conversion to a foreland-type depocentre. A simple examination of the basinal cross-section reveals a marked asymmetry, typical of foreland basins (e.g. DeCelles & Giles, 1996). The three-dimensional backstripping results (Fig. 9) also imply that the eastern Officer Basin developed at various times as an elongate sedimentary trough. Such a trough is produced by, and parallel to, an advancing orogen (Dickinson, 1974; Beaumont, 1981; Jordan, 1981). Its length is governed by the extent and geometry of the orogenic load (DeCelles & Giles, 1996) and its width by the flexural rigidity of the supporting lithosphere (Turcotte & Schubert, 1982; Watts, 1992). The normalized subsidence results (Fig. 9) show how the position of the depocentre has changed with time. With the exeption of the earliest period (M1), there is a marked asymmetry in the basin established at time-M2. As the initial basin-forming mechanisms involving broad regional subsidence remain obscure, the most significant tectonic event that determined subsequent basin architecture would have taken place in time-M2, clearly setting the pattern for future sedimentation in the basin. Overall, given the geological history of the Officer Basin and in light of the subsidence results, the basin can be thought of as being a polyphase foreland-type basin that was initiated as, and evolved from, a continental sag.

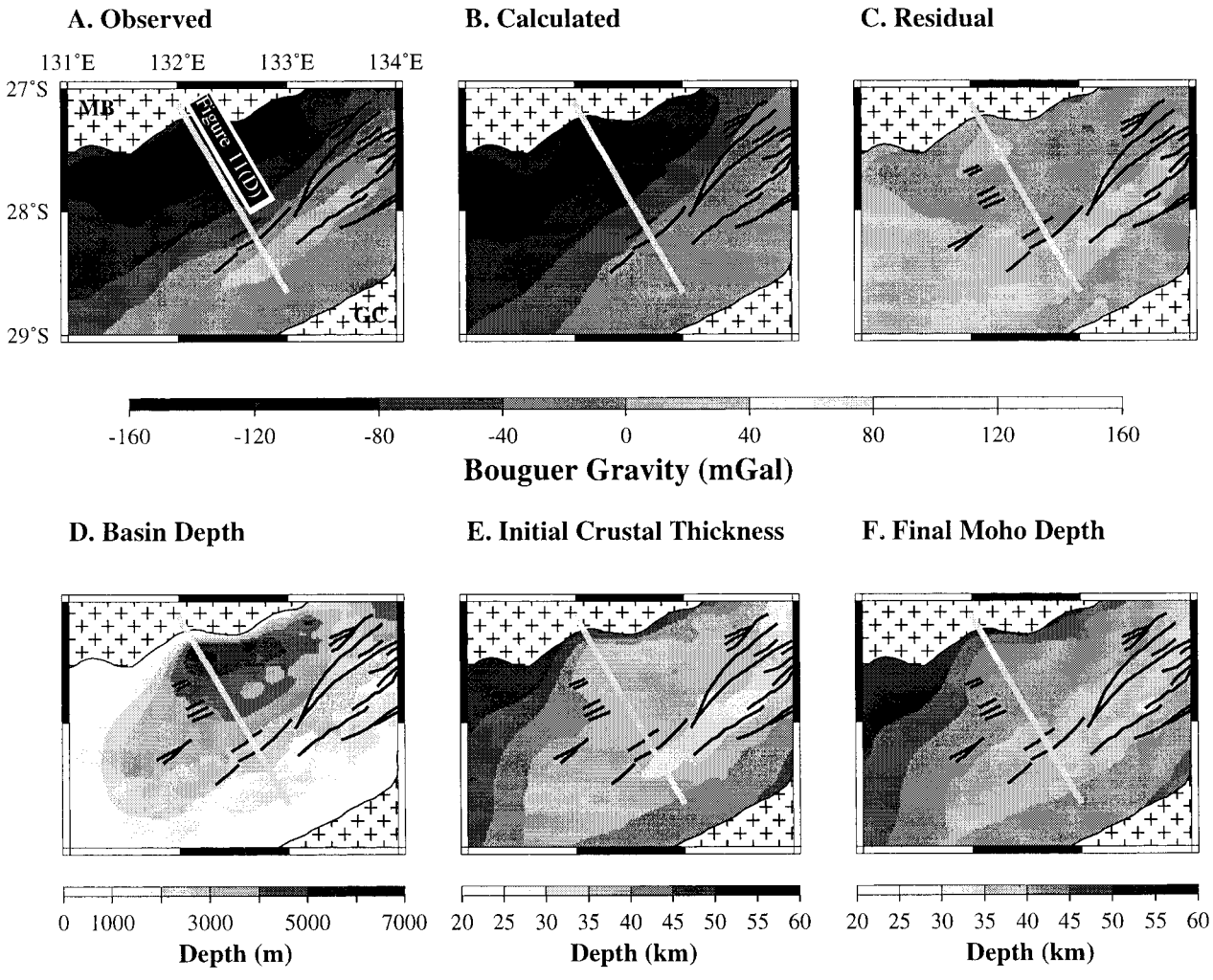

Fig. 12. Model results for equivalent crustal thickening/thinning beneath the eastern Officer Basin. The top row shows the effect of crustal thickness variations on the gravity field. The bottom row is an illustration of the crustal architecture before and after foreland-type loading. Note that the residual is reduced compared to Fig. 11, but not eliminated. The position of Fig. 13 is shown as a grey line.

The best fitting gravity model suggests there is an important component of flexure at the base of the crust that can produce the large, negative anomalies. In this sense, the Officer Basin is different from other commonly studied intracratonic basins, with perhaps the exception of the Ferghana Basin (Burov *et al.*, 1998), where crustal folding has resulted in large, negative Bouguer gravity anomalies. The contrasts with the Michigan, Illinois and Paraná basins is particularly striking since these basins are characterized by long-wavelength, small negative-amplitude gravity anomalies, with a superimposed high (Table 1).

A flexural model explains the persistence of these anomalies for long periods of time. Deep seismic data (e.g. Lindsay, 1995; Korsch *et al.*, 1998) do not provide evidence of rifting or for the emplacement of large, low-density bodies. Even in the simplest case, where the crust maintains a constant thickness through time, it is apparent that rifting of the basin fails to adequately explain its evolution. Rather, it may be that successive thrusting of the cratonic blocks in central Australia resulted in dismembering the continental-scale basin.

The calculated gravity anomalies that best satisfy the observed data are produced by models that significantly depress the Moho beneath the basin and also have a variable thickness crust. Numerous deep seismic profiles across central Australia (e.g. Goleby *et al.*, 1988; Korsch *et al.*, 1998; Wright *et al.*, 1990) point to a crust that shows some evidence of crustal thickening and mantle displacement by thick-skinned tectonics. Teleseismic results (Lambeck & Penney, 1984; Lambeck *et al.*, 1988) indicate significant Moho 'topography' beneath the region, even over short distances. Moreover, deep seismic studies from other shield areas show significant Moho depth variation. In the Urals, crustal thickness increases from the East European Platform to beneath the orogen (Knapp *et al.*, 1996). Diaconescu *et al.* (1998) determined a 5-km offset of the Moho in the same region and similar magnitudes have been recorded in the Baltic shield (BABEL Workinc Group, 1990).

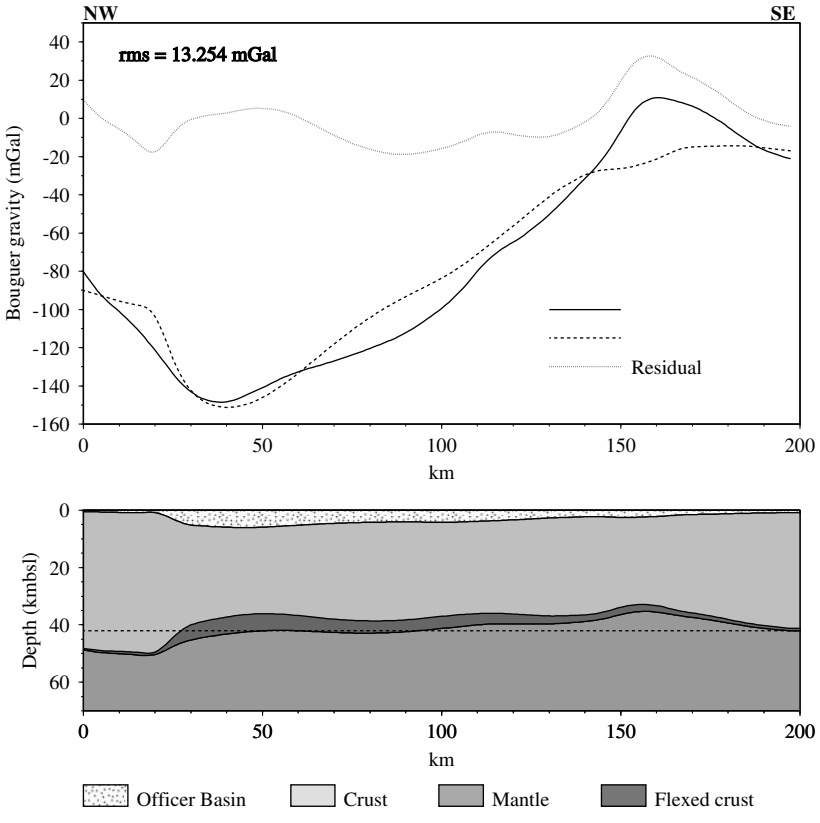

Fig. 13. Profiles taken from the gravity models for an initially variable thickness crust beneath the eastern Officer Basin. The proposed starting model is displayed in the lower figure. The dashed line in the lower figure is the position of the crust/mantle boundary due to warping of a constant thickness (42 km) crust. Note the reduction of the misfit in the upper figure, as reflected in the rms value and increase of the cc value. See Fig. 12 for location.

Table 1. Compilation of intracratonic basins showing the crustal structure and Bouguer gravity anomaly character. Parana data are sourced from Zalan *et al.* (1990) and Vidotti *et al.* (1998); Paris Basin from Brunet & Le Pichon (1982), Perrodon & Zabek (1990) and Cloetingh *et al.* (1999); Illinois Basin from Buschbach & Kolata (1990); Michigan Basin from Catacosinos *et al.* (1990); Williston Basin from Fowler & Nisbet (1985), Bond & Kominz (1991) and Nelson *et al.* (1993); Congo Basin from Daly *et al.* (1992); Ferghana Basin from Burov & Molnar (1998).

Basin	Crustal structure	Crustal thickness (km)	Crustal age (Ma)	Sediment age (Ma)	Gravity (mGal)
Officer	warp/foreland-type	41–48	1700–1075	>800–300	negative (up to ~ −150)
Amadeus	warp/foreland-type	41–50	2000–900	>800–300	negative (up to ~ −150)
Illinois	buried rift	39–45	1500–1420	570–0	central high (−30 to 20)
Michigan	buried rift	43	1500–900	530–0	central high (35 to 5)
Williston	antiform	41–48	up to 2000	520–0	central high (~ −100 to 0)
Paris	(?)warp/rift	35–40	570+	250–30	small central low (−45 to 20)
Parana	buried rift	40–45	700–450	415–65	central high (−100 to 50)
Congo	failed rift	?	1400–1000	670–2	negative (up to −150)
Ferghana	folded/warped	40–60	?	205+−0	central low (−260 to −200)

It has been suggested that these Moho offsets in some shield areas are the remnents of Archaean and Proterozoic tectonic processes, such as subduction and thus coincide with ancient terrane boundaries across which a different crustal thickness exists (Gibb & Thomas, 1976; BABEL Working Group, 1990; Calvert *et al.*, 1995; Diaconescu *et al.*, 1998). Certainly, the composite nature of the Williston Basin lithosphere is recognized (e.g. Green *et al.*, 1995). It has even been suggested that an ancient subduction zone (1.9–1.7 Gyr) once operated in central Australia (Zhao & McCulloch, 1995). Deep-seated fault planes that pre-date the Officer Basin and extend almost to the base of the crust are common beneath the Australian intracratonic basins (Lindsay, 1995; Lindsay & Leven, 1996). Thus the gravity model for the crust shown in Fig. 14 is a feasible representation of central Australia, where the gravity field may be in part a reflection of Archaean and Proterozoic structure. This further suggests that the long-term thermo-mechanical properties of lithosphere beneath the thick, stable continents are dominated by great strength (e.g. Karner *et al.*, 1983; Zuber *et al.*, 1989; Bechtel *et al.*, 1990) and can maintain stresses, and hence structure, over great spans of time. The general lack of isostatic compensation observed

in the Officer Basin may thus be explained, as has been done for the Redbank Thrust Zone at the northern margin of the Amadcus Basin (Beekman *et al*., 1997).

CONCLUSIONS

The Officer Basin in central Australia is an intracratonic basin characterized by an asymmetric and strongly negative gravity field. In view of the subsidence results and general architecture of the region, the present-day eastern Officer Basin most closely represents a foreland-type. The asymmetry of the basement, gravity anomalies and subsidence patterns, in the context of a multiple orogenic tectonic history, support this conclusion.

Despite its resemblance to a foreland basin, however, the origins of the Officer Basin remain obscure. It is apparently linked to other central Australian basins and was most likely initiated as part of a broad continental sag. It is possible that Proterozoic plume activity initiated continental-scale subsidence (i.e. M1), but much of the early sedimentary record has not been preserved. Gravity modelling of the eastern Officer Basin also supports a flexural evolution of the basin, even given two extensional epsiodes at time M1 and M4. The resultant crustal thinning from these events is not sufficient to negate the gravity low that is expected from a foreland-type basin. However, some thinning and thickening of the crust is required to explain the observed data. Deep seismic reflection and refraction data point to an undulating Moho beneath central Australia, a finding that is consistent with the gravity models. The best fitting gravity model is one in which a crust that is thickened towards the ancient orogen (north) and thinned away from it and flexurally deformed by a primarily vertically applied load.

It is unlikely that models of regional whole-crust warping are sufficient to explain the observed data. A simple comparison of Officer Basin subsidence to adjacent Amadeus Basin subsidence shows that the orogenies that were active in central Australia had different influences on the various basins. In the Officer Basin, orogenic deformation and modification may have occurred at an earlier time than it did in the Amadeus basin to the north. Later orogenic events that were important in the evolution of the Amadeus Basin were apparently of a more limited geographical extent in the Officer Basin. Therefore, beyond the earliest history of the central Australian basins (M1), when all were apparently connected in a broad continental sag, it would appear that the basins evolved separately, but within the context of continent-wide tectonics.

For central Australia to maintain a state of apparent isostatic disequilibrium over a long period of time suggests that the continent is strong and can support stresses over these periods. Alternatively, if rebound is occurring, it may be at very long, i.e. continental-scale, wavelengths, so that its effect is not readily observed in a basin that is only 200 km across. At present, there is no evidence of significant tectonic subsidence or uplift in central Australia, further pointing to the long-term strength of this part of the continental interior. Against the background of the subsidence results and preserved geological record, it is not unreasonable to assume that this has been the case for a long time.

ACKNOWLEDGMENTS

We are grateful to Jonathan Stewart for the provision of his three-dimensional gravity code. We also thank Rex Bates for his assistance with figure drafting.

REFERENCES

Athy, L.F. (1930) Density, porosity and compaction of sedimentary rocks. *Bull. Am. Ass. Petrol. Geol.*, **14**, 1–24.

Audet, D.M. (1995) Modelling of porosity evolution and mechanical compaction of calcareous sediments. *Sedimentology*, **42**, 355–373.

Babel Workinc Group. (1990) Evidence for early Proterozoic plate tectonics from seismic reflection profiles in the Baltic shield. *Nature*, **348**, 34–38.

Baldwin, B. & Butler, C.O. (1985) Compaction curves. *Bull. Am. Ass. Petrol. Geol.*, **69**, 622–626.

Beaumont, C. (1981) Foreland basins. *Geophys. J. R. Astron. Soc*., **65**, 291–329.

Bechtel, T.D., Forsyth, D.W., Sharpton, V.L. & Grieve, R.A. (1990) Variations in effective elastic thickness of the North American lithosphere. *Nature*, **343**, 636–638.

Beekman, E., Stephenson, R.A. & Korsch, R.J. (1997) Mechanical stability of the Redbank Thrust Zone, central Australia: dynamic and rheological implications. *Aust. J. Earth Sci.*, **44**, 215–226.

Bond, G. C. & Kominz, M.A. (1991) Disentangling middle Paleozoic sea level and tectonic events in cratonic margins and cratonic basins of North America. *J. Geophys. Res.*, **96**, 6619–6639.

Bond, G.C., Nickeson, P.A. & Kominz, M.A. (1984) Breakup of a supercontinent between 625 Ma and 555 Ma; new evidence and implications for continental histories. *Earth Planet. Sci. Lett.*, **70**, 325–345.

Brunet, M.-F. & Le Pichon, X. (1982) Subsidence of the Paris Basin. *J. Geophys. Res.*, **87**, 8547–8560.

Burov, E.B. & Diament, M. (1998) The effective elastic thickness (T_e) of continental lithosphere: what does it really mean? *J. Geophys. Res.*, **100**, 3905–3927.

Burov, E.B. & Molnar, P. (1998) Gravity anomalies over the Ferghana Valley (central Asia) and intracontinental deformation. *J. Geophys. Res.*, **103**, 18137–18152.

Buschbach, T.C. & Kolata, D.R. (1990) Regional setting of Illinois Basin. In: *Interior Cratonic Basins* (Ed. by W. Leighton, D. R. Kolata, D. E. Oltz & J. J. Eidel), *Am. Ass. Petrol. Geol. Mem*., **51**, 29–55.

Calvert, A.L., Sawyer, E.W., Davis, W.J. & Ludden, J.N. (1995) Archaean subduction inferred from seismic images of a mantle suture in the superior province. *Nature*, **375**, 670–674.

Cartwright, I. & Buick, I.S. (1999) The flow of surface derived fluids through Alice Springs age middle-crustal ductile shear zones, Reynolds Range, central Australia. *J. Metamorphic Geol.*, **17**, 397–414.

Catacosinos, R.A., Daniels, P.A. & Harrison, W.B. (1990) Structure, stratigraphy, and petroleum geology of the Michigan Basin. In: *Interior Cratonic Basins* (Ed. by M. W. Leighton, D. R. Kolata, D. E. Oltz & J. J. Eidel), *Am. Ass. Petrol. Geol. Mem.*, **51**, 561–601.

Cloetingh, S., Burov, E. & Poliakov, A. (1999) Lithosphere folding: Primary response to compression? (from central Asia to Paris basin). *Tectonics*, **18**, 1064–1083.

Cloetingh, S. & Wortel, R. (1986) Stress in the Indo-Australian Plate. *Tectonophysics*, **132**, 49–67.

Comacho, A. & McDougall, I. (2000) Intracratonic strike-slip partitioned transpression and the formation and exhumation of eclogite facies rocks: an example from the Musgrave Block, central Australia. *Tectonics*, **19**, 978–996.

Daly, M.C., Lawrence, S.R., Diemu-Tshiband, K. & Matouana, B. (1992) Tectonic evolution of the Cuvette Centrale, Zaire. *J. Geol. Soc. Lond.*, **149**, 539–546.

Decelles, P.G. & Giles, K.A. (1996) Foreland basin systems. *Basin Res.*, **8**, 105–123.

DeRito, R.E., Cozzarelli, F.A. & Hodge, D.S. (1983) Mechanisms of subsidence of ancient cratonic rift basins. *Tectonophysics*, **94**, 141–168.

Dewey, J.F. (1982) Plate tectonics and the evolution of the British Isles. *J. Geol. Soc. Lond.*, **139**, 371–412.

Diaconescu, C.C., Knapp, J.H., Brown, L.D., Steer, D.N. & Stiller, M. (1998) Precambrian Moho offset and tectonic stability of the East European platform from the URSEIS deep seismic profile. *Geology*, **26**, 211–214.

Dickinson, W.R. (1974) Plate tectonics and sedimentation. In: *Plate Tectonics and Sedimentation* (Ed. by W. R. Dickinson), *Spec. Publ. Soc. Econ. Palaeont. Miner.*, **22**, 1–27.

Fowler, C.M.R. & Nisbet, E.G. (1985) The subsidence of the Williston Basin. *Can. J. Earth Sci.*, **22**, 408–415.

Gibb, R.A. & Thomas, M.D. (1976) Gravity signature of fossil plate boundaries in the Canadian Shield. *Nature*, **262**, 199–200.

Goleby, B.R., Shaw, R.D., Wright, C., Kennett, B.L.N. & Lambeck, K. (1989) Geophysical evidence for 'thick-skinned' crustal deformation in central Australia. *Nature*, **337**, 325–330.

Goleby, B.R., Wright, C., Collins, C.D.N. & Kennett, B.L.N. (1988) Seismic reflection and refraction profiling across the Arunta Block and the Ngalia and Amadeus basins. *Aust. J. Earth Sci.*, **35**, 275–294.

Gravestock, D.I. & Hibburt, J.E. (1988) Sequence stratigraphy of the Eastern Officer and Arrowie basins: a framework for Cabrian oil search. *J. Aust. Petrol. Expl. Ass.*, **31**, 177–190.

Green, J.C. (1983) Geological and geochemical evidence for the nature and development of the middle Proterozoic (Keweenawan) mid-continent rift of North America. *Tectonophysics*, **94**, 413437.

Green, A.G., Weber, W. & Hajnal, Z. (1985) Evolution of Proterozoic terrains beneath the Williston Basin. *Geology*, **13**, 624–628.

Grotzinger, J. & Royden, L. (1990) Elastic strength of the Slave craton at 1.9 Gyr and implications for the thermal evolution of the continents. *Nature*, **347**, 64–66.

Haddad, D. & Watts, A.B. (1999) Subsidence history, gravity anomalies and flexure of the northeast Australian margin in Papua New Guinea. *Tectonics*, **18**, 827–842.

Hand, M., Mawby, J., Kinny, P. & Foden, J. (1999) U–Pb ages from the Hart's Range, central Australia: evidence for early Ordovician extension and constraints on Carboniferous metamorphism. *J. Geol. Soc. Lond.*, **156**, 715–730.

Hocking, R.M., Mory, A.J. & Williams, 1. R. (1994) An atlas of Neoproterozoic and Phanerozoic basins of Western Australia (1994). In: *The Sedimentary Basins of Western Australia: Proceedings of Petroleum Exploration Society of Australia Symposium* (Ed. by P. G. Purcell & R. R. Purcell), pp. 21–43. Petrol. Expl. Soc. Aust.

Jordan, T. (1981)Thrust loads and foreland basin evolution. *Bull. Am. Ass. Petrol. Geol.*, **65**, 2506–2520.

Karlstrom, K.E., Harlan, S.S., Williams, M.L., Mclelland, L., Geissman, J.W. & Ahäll, K-I. (1999) Refining Rodinia: geologic evidence for the Australia–western U.S. connection in the Proterozoic. *GSA Today*, **9**, 1–7.

Karner, G.D., Steckler, M.S. & Thorne, J.A. (1983) Long-term thermo-mechanical properties of the continental lithosphere. *Nature*, **304**, 250–253.

Knapp, J.H., Steer, D.N., Brown, L.D., Berzin, R., Suleimanovember, A., Stiller, M., Lueschen, E., Brown, D.L., Bulgakov, R., Kashubin, S.N. & Rybalka, A.V. (1996) Lithospheric scale seismic image of the southern Urals from explosion-source reflection profiling. *Science*, **274**, 226–228.

Korsch, R.L., Goleby, B.R., Leven, J.H. & Drummond, B.J. (1998) Crustal architecture of central Australia based on deep seismic reflection profiling. *Tectonophysics*, **288**, 57–69.

Lambeck, K. (1983) Structure and evolution of the intracratonic basins of central Australia. *Geophys. J. R. Astron. Soc.*, **74**, 843–886.

Lambeck, K., Burgess, G. & Shaw, R.D. (1988) Teleseismic travel-time anomalies and deep crustal structure in central Australia. *Geophys. J.*, **94**, 105–124.

Lambeck, K. & Penney, C. (1984) Teleseismic travel time anomalies and crustal structure in central Australia. *Phys. Earth Planet. Interiors*, **34**, 46–56.

Lindsay, J.F. (1987) Sequence stratigraphy and depositional controls in late Proterozoic-Early Cambrian sediments of Amadeus Basin, central Australia. *Bull. Am. Ass. Petrol. Geol.*, **71**, 1387–1403.

Lindsay, J.F. (1995) *Geological Atlas of the Officer Basin, South Australia*. Australian Geological Survey Organisation and Department of Mines and Energy, South Australia, 30 plates.

Lindsay, J.F. (1999a) The Heavitree quartzite, a Neoproterozoic (c. 800–760 Ma), high-energy, tidally influenced, ramp association, Amadeus Basin, central Australia. *Aust. J. Earth Sci.*, **46**, 127–149.

Lindsay, J.F. (1999b) *Geological Atlas of the Officer Basin, South Australia (CD-ROM edition)*. Australian Geological Survey Organisation Record 1999/43, 30 plates.

Lindsay, J.F. & Korsch, R.J. (1989) Interplay of tectonics and sea level changes in basin evolution: an example from the intracratonic Amadeus Basin, central Australia. *Basin Res.*, **2**, 3–25.

Lindsay, J.E., Korsch, R.J. & Wilford, J.R. (1987) Timing the breakup of a Proterozoic supercontinent: evidence from Australian intracratonic basins. *Geology*, **15**, 1061–1064.

Lindsay, J.F. & Leven, J.H. (1996) Evolution of a Neoproterozoic to Palaeozoic intracratonic setting, Officer Basin, South Australia. *Basin Res.*, **8**, 403–424.

Lowry, A.R. & Smith, R.B. (1996) Strength and rheology of the western U.S. Cordillera. *J. Geophys. Res.*, **100**, 17947–17963.

Maboko, M.A.H., McDougall, I., Zeitler, P.K. & Williams, 1. S. (1992) Geochronological evidence for – 530–550 Ma juxtaposition of two Proterozoic metamorphic terranes in the Musgrave Ranges, central Australia. *Aust. J. Earth Sci.*, **39**, 457–471.

Madon, M.B. & Watts, A.B. (1998) Gravity anomalies, subsidence history and the tectonic evolution of the Malay and Penyu Basins (offshore Peninsula Malaysia). *Basin Res.*, **10**, 375392.

Mathews, S.C. & Cowie, J.W. (1979) Early Cambrian transgressions. *J. Geol. Soc. Lond.*, **136**, 133–135.

Mathur, S.R. (1977) Gravity anomalies and crustal structure-a review. *Bull. Aust. Soc. Expl. Geophys.*, **8**, 111–117.

Mcadoo, D.C. & Sandwell, D.T. (1985) Folding of oceanic lithosphere. *J. Geophys. Res.*, **90**, 8563–8569.

McQueen, H.W.S. & Beaumont, C. (1989) Mechanical models of tilted block basins. In: Origin and Evolution of Sedimentary Basins and Their Mineral Resources (Ed. by R. A. Price), *AGU/IUGG Monograph*, **48**, 65–71.

Moussavi-Harami, R. & Gravestock, D., (1995) 1. Burial history of the eastern Officer Basin, South Australia. *Bull. Aust. Petrol. Expl. Ass.*, **35**, 307–320.

Nelson, K.D., Baird, D.L., Walters, J.L., Hauck, M., Brown, L.D., Oliver, J.E., Ahern, J.L., Hmnal, Z., Jones, A.G. & Sloss, L.L. (1993) Trans-Hudson orogen and 33 williston basin in Montana and North Dakota: New COCORP deep-profiling results. *Geology*, **21**, 447–450.

Perrodon, A. & Zabek, J. (1990) Paris Basin. In: *Interior Cratonic Basins* (Ed. by M. W. Leighton, D. R. Kolata, D. F. Oltz & J. J. Eidel), *Am. Ass. Petrol. Geol. Mem.*, **51**, 633–679.

Piper, J.D.A. (1983) Proterozoic palaeomagnetism and single continent plate tectonics. *Geophys. J. R. Astron. Soc.*, **74**, 163–197.

Plumb, K.A. (1979) The tectonic evolution of Australia. *Earth Sci. Rev.*, **14**, 205–249.

Powell, C.M., Priess, M.V., Gatehouse, C.G., Krapez, B. & Li, Z.X. (1994) South Australian record of a Rodinian epicontinental basin and its mid-Neoproterozoic breakup (-700 Ma) to form the Palaeo-Pacific Ocean. *Tectonophysics*, **237**, 113–140.

Preiss, W.V. & Forbes, B.G. (1981) Stratigraphy, correlation and sedimentary history of Adelaidean (Late Proterozoic) basins in Australia. *Precamb. Res.*, **15**, 255–304.

Royer, L.-Y. & Gordon, R.G. (1997) The motion and boundary between the Capricorn and Australian plates. *Science*, **277**, 1268–1274.

Shaw, R.D., Etheridge, M.A. & Lambeck, K. (1991) Development of the Late Proterozoic to mid-Palaeozoic, intracratonic Amadeus Basin in central Australia: a key to understanding tectonic forces in plate interiors. *Tectonics*, **10**, 688–721.

Stephenson, R. & Lambeck, K. (1985) Isostatic response of the lithosphere with in-plane stress: application to central Australia. *J. Geophys. Res.*, **90**, 8581–8588.

Sukanta, U. (1993) Sedimentology, sequence stratigraphy and palaeogeography of marinoan sediments in the eastern Officer Basin, South Australia. PhD thesis, Flinders University of South Australia.

Turcotte, D.L. & Schubert, G. (1982) *Geodynamics: Applications of Continuum Physics to Geological Problems*. John Wiley and Sons, New York.

Vail, P.R., Mitchum, R.M. & Thompson, S. (1977) Seismic stratigraphy and global changes of sea level, part 3: relative changes of sea level from coastal onlap. In: *Stratigraphy – Application to Hydrocarbon Exploration* (Ed. by C. E. Payton), *Am. Ass. Petrol. Geol. Mem.*, **26**, 63–81.

Veevers, J.J. & Welhinny, M.W. (1976) The separation of Australia from other continents. *Earth Sci. Rev.*, **12**, 139–159.

Vidotti, R.M., Ebinger, C.J. & Fairhead, J.D. (1998) Gravity signature of the western Parand Basin, Brazil. *Earth Planet. Sci. Lett.*, **159**, 117–132.

Walter, M.R., Veevers, J.L., Calver, C.R., Grey, K. & Hilyard, D. (1992) The Proterozoic Centralian Superbasin: a frontier petroleum province. *Bull. Am. Ass. Petrol. Geol.*, **76**, 1132.

Walter, M.R. & Gorter, J.D. (1994) The Neoproterozoic Centralian Superbasin in Western Australia. In: *The Sedimentary Basins of Western Australia: Proceedings of the Petroleum Exploration Society of Australia Symposium* (Ed. by P. G. Purcell & R.R. Purcell), pp. 851–964. Petrol. Expl. Soc. Aust.

Walter, M.R., Grey, K., Williams, I.R. & Calver, C.R. (1994) Stratigraphy of the Neoproterozoic to early Palaeozoic Savory Basin, Western Australia, and correlation with the Amadeus and Officer basins, Australia. *Aust. J. Earth Sci.*, **41**, 533–546.

Walter, M.R., Veevers, J.L., Calver, C.R. & Grey, K. (1995) Neoproterozoic stratigraphy of the Centralian Superbasin, Australia. *Precamb. Res.*, **73**, 173–195.

Watts, A.B. (1978) An analysis of isostasy in the world's oceans 1: Hawaiian–Emperor seamount chain. *J. Geophys. Res.*, **83**, 5989–6004.

Watts, A.B. (1988) Gravity anomalies, crustal structure and flexure of the lithosphere at the Baltimore Canyon Trough. *Earth Planet. Sci. Lett.*, **89**, 221–238.

Watts, A.B. (1992) The effective elastic thickness of the lithosphere and the evolution of fore∼ land basins. *Basin Res.*, **4**, 169–178.

Weissel, J.K., Anderson, R.N. & Geller, C.A. (1980) Deformation of the IndoAustralian Plate. *Nature*, **287**, 284–291.

Wellman, P. (1982) Australian seismic refraction results, isostasy and altitude anomalies. *Nature*, **298**, 838–841.

Wingate, M.T.D., Campbell, I.H., Compston, W. & Gibson, G.M. (1998) Ion microprobe U-Pb ages for Neoproterozoic basaltic magmatism in south-central Australia and implications for the breakup of Rodinia. *Precamb. Res.*, **87**, 135–159.

Wright, C., Goleby, B.R., Collins, C.D.N., Korsch, R.L., Barton, T., Green-Halgh, S.A. & Sugmarto, S. (1990) Deep seismic profiling in central Australia. *Tectonophysics*, **173**, 247–256.

Zalán, P.V., Wolff, S., Astolfi, M.A.M., Vieira, I.S., Cão, J.C., Appi, V.T., Neto, E.V.S., Cerqueira, J.R. & Marques, A. (1990) The Parand Basin, Brazil. In: Interior Cratonic Basins (Ed. by W. Leighton, D. R. Kolata, D. E. Oltz & J. J. Eidel), *Am. Ass. Petrol. Geol. Mem.*, **51**, 681–708.

Zhao, J.X. & McCulloch, M.T. (1993) Sm–Nd mineral isochron ages of Late Proterozoic dyke swarms in Australia: evidence for two distinctive events of mafic magmatism and crustal extension. *Chem. Geol.*, **109**, 341–354.

Zhao, J.X. & McCulloch, M.T. (1995) Geochemical and Nd isotopic systematics of granites from the Arunta Inlier,

central Australia: implications for Proterozoic crustal evolution. *Precamb. Res.*, **71**, 265–299.

Zhao, J.X., McCulloch, M.T. & Korsch, R.J. (1994) Characteristic of a plume-related – 800 Ma magmatic event and its implications for basin formation in central-southern Australia. *Earth Planet. Sci. Lett.*, **121**, 349–367.

Zoback, M.D., Stephenson, R.A., Cloetingh, S., Larsen, B.T., Hoorn, B.V., Robinson, A., Horvath, F., Pumdefabregas, C. & Ben-Avraham, Z. (1993) Stresses in the lithosphere and sedimentary basin formation. *Tectonophysics*, **226**, 1–13.

Zuber, M.T., Bechtel, T.D. & Forsyth, D.W. (1989) Effective elastic thickness of the lithosphere, and mechanisms of isostatic compensation in Australia. *J. Geophys. Res.*, **94**, 9353–9367.

Received 8 July 2000; revision accepted 31 January 2001

